ANNEALING OF QUENCHED-IN VACANCIES IN ALUMINIUM—0.1 Wt.% CHROMIUM ALLOY

By
NARENDRA KUMAR GARG

DEPARTMENT OF METALLURGICAL ENGINEERING
INDIAN INSTITUTE OF TECHNOLOGY KANPUR
JANUARY, 1976

ANNEALING OF QUENCHED-IN VACANCIES IN ALUMINIUM—0.1 Wt.% CHROMIUM ALLOY

By
NARENDRA KUMAR GARG

DEPARTMENT OF METALLURGICAL ENGINEERING
INDIAN INSTITUTE OF TECHNOLOGY KANPUR
JANUARY, 1976

CERTIFICATE

This is to certify that the work ANNEALING OF QUENCHED-IN VACANCIES IN ALUMINIUM - 0.1 wt % CHROMIUM ALLOY has been carried out by Mr. Narendra Kumar Garg under my supervision and that it has not been submitted elsewhere for a degree.

(T.R. Ramachandran)
Assistant Professor
Department of Metallurgical Engineerir
Indian Institute of Technology
Kanpur-208016 U.P. INDIA

ACKNOWLEDGEMENT

The author is deeply indebted to Dr. T.R. Ramachandran, his thesis supervisor, for painstaking guidance and encouragement throughout the research program.

The valuable and crucial assistance provided by Mr. Nirbhay Singh is gratefully acknowledged.

Thanks are due to fellow graduate students Mr. Jogendra singh and Mr. B.P. Kashyap for their co-operations and assistance.

The author thanks Mr. K.P. Mukherjee, Mr. H.C. Srivastava for sundry help offered during the experimental stages of the work. The author is grateful to Mr. R.N. Srivastava for an excellent typing job.

TABLE OF CONTENTS

LIST OF TABLES

LIST OF FIGURES

SYNOPSIS

ANNEALING OF QUENCHED-IN VACANCIES IN ALUMINIUM - 0.1 wt % CHROMIUM ALLOY

The object of the present investigation is to determine the chromium-vacancy binding energy in aluminium by studying the decay of quenched-in vacancies in aluminium - 0.1 wt % chromium alloy. The process of decay is followed by electrical resistivity measurements at liquid nitrogen temperature.

Two stages of recovery are observed when both pure aluminium and the aluminium-chromium alloy are quenched from 500°C and isochronally annealed in the temperature range 0 to 240°C. The first recovery stage lies in the temperature range 0 to 40°C and the second between 120 to 240°C. From the results obtained it is difficult to draw any conclusions about the effect of chromium on the isochronal annealing behaviour of quenched aluminium. Isothermal annealing measurements are carried out in the temperature range 0 to 30°C on both the materials quenched from 500°C. The resulting annealing data do not, in general, conform to first or second order kinetics, although the low temperature annealing (0 and 10°C) data could be fitted to a second

order reaction. The isothermal annealing data for the alloys are analysed, on the basis of a model which takes into account the simultaneous annealing of single and divacancies, to give a value of 0.13 to 0.17 eV for the chromium-vacancy binding energy.

When the alloy is quenched from 500°C and then isothermally annealed at 250°C, there is a significant decrease in resistivity of the order of 150 n ohm cm in about 1200 minutes, after which no further change in resistivity occurs. Probably precipitation of chromium is occurring at this temperature however, this is to be checked by other experimental methods.

CHAPTER 1

INTRODUCTION

Several of the physical and mechanical properties of metallic crystals are controlled by the presence of imperfections. The latter can be classified as follows:

1. Point defects - vacancies, interstitials and impurity (or solute) atoms
2. Line defects - dislocations
3. Area defects - grain boundaries, surfaces and stacking faults
4. Volume defects - voids or pores, precipitates.

Of these defects, point defects are the only species which are in thermodynamic equilibrium. The others are accidents of growth of the crystals and under favourable conditions can be minimised. An excess concentration of point defects can be produced in metallic materials by quenching from elevated temperatures, plastic deformation, nuclear irradiation or deviation from stoichiometric composition.

Point defects can interact with one another. A vacancy can combine with another vacancy to form a divacancy. A vacancy and an interstitial can react

resulting in an atom in the normal lattice site; in this process both the defects are eliminated. The formation of trivacancy, tetra vacancies, diinterstitials and other complex clusters can be easily visualised under suitable conditions. These clusters may assume large size leading to the formation of dislocation loops or voids.

Impurities or solute atoms also interact with vacancies to form solute-vacancy complexes or bound vacancies. The importance of this interaction was first indicated by Johnson in 1939[1] in connection with diffusion in dilute alloys. The concentration of the solute-vacancy complexes depends on the magnitude of the solute-vacancy binding energy, B_{Vi}, which is defined as the difference between the energies required for the formation of a vacancy in the solute free-lattice and in a site which has only one solute atom in its nearest neighbouring position. For positive values of binding energy the equilibrium concentration of vacancies in a pure solvent is less than that in the alloy at the same temperature, the exact difference being a function of temperature, solute concentration and binding energy.

Whenever excess point defects are present in a pure metal or alloy, there is a tendency for the former to move to sinks and get destroyed there until the

concentration of the defects is reduced to that characteristic of the temperature. This process of elimination of excess defects is called annealing. Experimental studies on the annealing of vacancies retained by a rapid quench from a high temperature have been widely carried in the last two decades using electrical resistivity measurements. The study of the temperature dependence of the concentration of vacancies in metals and alloys leads to the estimation of the formation energy of a vacancy in the pure metal and the solute-vacancy binding energy (thermodynamic method). The migration energy of a vacancy and the solute-vacancy binding energy can be estimated by studying the rate of decay of excess of vacancies in the pure metal and the alloy (kinetic method). The sum of the formation and migration energies of a vacancy must be equal to the activation energy of diffusion, if diffusion occurs by vacancy mechanism.

Quenched-in vacancies play a prominent role in influencing the initial stages of precipitation in supersaturated alloys. For example, if the solute-vacancy complex is slow moving, precipitation can be sluggish. The clusters of vacancies such as dislocation loops and voids can act as sites for heterogeneous nucleation of the precipitates. A large number of investigations have been

carried out on the behaviour of quenched-in vacancies in several aluminium-base alloys. The results of several of these investigations are summarized by Federighi[2]. Recent studies on the diffusion of transition elements (Mn, Cr, Ni, Fe) in aluminium indicates anomalously high activation energies for solute diffusion[3]. As the investigations on the behaviour of excess vacancies in aluminium-transition metal alloys are limited, we have started systematic studies on Al-Mn, Al-Cr and Al-Fe alloys. The results obtained on the annealing of excess vacancies in an Al - 0.1 wt % Cr alloy are presented in this thesis. Electrical resistivity measurements are used to carry out the necessary investigations.

CHAPTER 2

REVIEW OF PREVIOUS WORK

It is now well established that vacancies and interstitials play a dominant role in the process of diffusion. The presence of excess vacancies can lead to enhanced diffusion. In the early stages of ageing of a precipitation hardening alloy, the rapid movement of solute atoms is brought about by the quenched-in vacancies. The clustering of the vacancies lead to the formation of defects like voids and dislocation loops which offer sites for the heterogeneous nucleation of precipitates. The thermodynamics of the point defects and the kinetics of annealing of excess defects are discussed in this chapter. The application of the kinetic principles to the study of solute-vacancy interaction in aluminium alloys is also elucidated.

2.1 THERMODYNAMICS OF VACANCIES IN METALS:

The formation of point defects in a crystal requires a certain amount of positive work which increases the internal energy of the crystal. However, the configurational or mixing entropy is also increased because there

are many ways of distributing the point defects among the available lattice sites. The Gibb's free energy is a minimum for a certain concentration of defects determined by the balance of the energy and entropy terms and this gives rise to the equilibrium concentration of vacancies at any temperature above 0°K.

Consider N atomic sites in which n vacancies are to be arranged. W, the number of ways in which they can be arranged is

$$W = \frac{N!}{(N-n)!\, n!} \tag{2.1}$$

The configurational entropy S, is given by the relation from statistical mechanics as

$$S = k \ln W = k \ln \frac{N!}{(N-n)!\, n!} \tag{2.2}$$

where k is the Boltzmann's constant.

Applying Stirling's approximation viz.

$$\ln x! = x \ln x - x, \quad \text{for } x \gg 1 ,$$

We get

$$S = k \left[N \ln N - (N-n) \ln (N-n) - n \ln n \right] \tag{2.3}$$

If E_V^f is the energy for the formation of a vacancy, then the increase in free energy, ΔG of a crystal

in forming n vacancies is given by

$$\Delta G = nE_V^f - TS \tag{2.4}$$

$$= nE_V^f - kT\left[N \ln N - (N-n) \ln(N-n) - n \ln n\right] \tag{2.5}$$

When we have the equilibrium no. of vacancies

$$\left(\frac{\partial \Delta G}{\partial n}\right) = 0 \tag{2.6}$$

From these considerations, we can show that

$$\frac{n}{(N-n)} = \exp\left[-\frac{E_V^f}{kT}\right] \tag{2.7}$$

since $n << N$, it can be neglected in the denominator of L.H.S. of equation (2.7).

In deriving the above equation, we have considered only the configurational entropy. The other entropy terms can be included by the introduction of a pre-exponential constant,

$$C_V = \frac{n}{N} = A \exp\left[-E_V^f/kT\right] \tag{2.8}$$

where C_V is the atomic concentration of vacancies and A is a constant. From this expression, it is clear that $C_V = 0$ at 0°K and C_V increases exponentially with temperature.

In a similar manner, we can calculate the equilibrium concentration of divancies. If the coordination

number of lattice is Z, there are ZN/2 adjacent pairs of lattice sites; n_2 divacancies can be distributed amongst these sites in the following number of ways

$$W = \frac{(ZN/2)!}{(ZN/2 - n_2)!\, n_2!} \qquad (2.9)$$

Proceeding as before, we can show that the divacancy concentration, C_{2V}, is

$$C_{2V} = \frac{n_2}{N} = \frac{1}{2} Z(C_V)^2 \exp(B_2/kT) \qquad (2.10)$$

where B_2 is the binding energy of a divanancy which is defined as $2E_V^f - E_{2V}^f$, where E_{2V}^f is the energy of formation of a divacancy.

2.2 FORMATION OF SOLUTE-VACANCY PAIRS:

In a dilute binary alloy, an interaction can exist between a solute atom and a vacancy occupying nearest neighbour positions. This interaction energy or the solute-vacancy binding energy, B_{Vi}, is defined as the difference in the energy of formation of a vacancy in a site having only solvent atoms as nearest neighbours and that in a site which has one solute atom in the first co-ordination shell. When B_{Vi} is positive, it is energetically favourable for

the vacancies to form next to the solute atoms, a tendency opposed by entropy consideration.

Vacancies in an impure metal can be either free or bound. Bound vacancy has one solute atom in its first co-ordination shell, free vacancy has all solvent atoms in its first co-ordination shell. The total vacancy concentration, C_V', in an alloy or impure metal is the sum of free vacancy concentration, C_V, and the bound vacancy concentration, C_{Vi}. Following Lomer[4], these are given by,

$$C_V = A(1 - \overline{Z+1}\, I_o) \exp(- E_V^f/kT) \qquad (2.11)$$

and

$$C_{Vi} = A\, Z\, I_o \exp\left[-(E_V^f - B_{Vi})/kT\right] \qquad (2.12)$$

where Z is the co-ordination number, I_o is the impurity concentration (atomic), A is the entropy factor, assumed to be the same for both free and bound vacancies, and E_V^f is the energy of formation of a vacancy in the pure solvent.

The total vacancy concentration, C_V', is given by the addition of equations (2.11) and (2.12).

$$C_V' = A \exp(- E_V^f/kT) \left[1 - \overline{Z+1}\, I_o + ZI_o \exp(B_{Vi}/kT)\right]$$

$$= C_V \left[1 - \overline{Z+1}\, I_o + ZI_o \exp(B_{Vi}/kT)\right] \qquad (2.13)$$

Equation (2.13) indicates that the total vacancy concentration in an alloy is greater than that in pure metal by an amount which depends on B_{Vi}, I_o and T. The ratio of the bound to the free vacancies increases with increase in B_{Vi} and decrease in temperature.

The binding energy of a solute to a vacancy is due to a strain energy term, ΔB_S, and an electrostatic interaction term, ΔB_C. The presence of large sized solute atom causes strain in the lattice which can be relieved by the presence of a vacancy adjacent to it. This can qualitatively account for the term ΔB_S. The electrostatic interaction term can arise when the impurity atom has a valency different from that of the solvent atom. In particular if the impurity atom has a higher valency, it attracts a vacancy by its side in order to minimise the electrostatic potential of the system.

2.3 QUENCHED-IN VACANCIES IN METALS:

A high concentration of vacancies can be retained in a metallic sample by soaking it at a high temperature, T_q, and then cooling it rapidly to a low temperature, T_a. The choice of T_q, T_a and β, the rate of quenching is very important in controlling the concentration of the excess vacancies. T_q must be high enough so that the concentration

of vacancies retained is large enough for precise measurement. But the degree of clustering of the defects increases with increase in T_q. If unassociated or unclustered defects are the only species of interest, this clustering process puts an upper limit to the quench temperature while measurable amount puts the lower limit.

Concentration of vacancy clusters (divacancies, trivacancies, etc.) increase at the expense of single vacancies during the quenching process. The concentrations of these clusters depend on their binding energy. When only single and divacancies are considered, there is a critical temperature, T*, below which equilibrium between C_V and C_{2V} is frozen during quenching. For aluminium, this critical temperature, T*, is defined by the equation[5]

$$\frac{7k\nu_3}{B_2\beta} = \frac{\exp((E_m + B_2)/kT^*)}{(1 + 480C_V^* \exp(B_2/kT^*))^{\frac{1}{2}}} \qquad (2.14)$$

where E_m is the migration energy of single vacancy, ν is the vibrational frequency of atoms which are the nearest neighbours of a vacancy and C_V^* is the single vacancy concentration at T*. It has been found out that the number of divacancies formed during quenching increases with an increase in quenching temperature and divacancy binding energy and with decreasing quenching rate[6]. When an

alloy is quenched the equilibrium between single vacancies, divacancies and bound vacancies can change with decrease in temperature. This problem has been studied in detail by Doyama[7]. If the solute-vacancy binding energy is higher than that for the divacancy and the solute concentration is higher than the single vacancy concentration, the reestablishment of equilibrium involves essentially single and bound vacancies. There is a critical temperature, T_a^*, below which the equilibrium between single vacancies and complexes is frozen, T_a^*, is defined by the expression[7]:

$$(\beta)_{T_a^*} = - \frac{7k\nu (T_a^*)^2}{B_{Vi}} \exp(- E_m/kT_a^*) \left[ZI_o + ZC_V^* \exp(B_{Vi}/kT_a^*)\right] \quad (2.15)$$

As with pure metals the concentration of single vacancies decreases during quenching.

2.4 KINETICS OF ANNEALING OF QUENCHED-IN VACANCIES:

It has already been pointed out that quenched-in vacancies can be retained only at sufficiently low temperature. If the temperature is raised appreciably, the excess vacancies migrate to the sinks so as to establish the concentration characteristic (equilibrium) of that temperature. The annealing of vacancies is the process

of disappearance of the super saturation of defects. Since the mobility of defects increases rapidly with increasing temperature, a suitable temperature interval can always be found in which the rate of disappearance of a given defect can be measured.

The annealing stages can be established by carrying out isochronal annealing on a quenched sample by heating it to successively higher temperatures in steps for constant time with attendent changes in vacancy concentration measured at the end of each step. The changes in vacancy concentration are found out by measuring the changes in a suitable physical property (normally electrical resistivity) of the quenched sample.

2.4.1 Isochronal Annealing:

Federighi et al[2,8] have reported the results of isochronal annealing of quenched 99.995% pure aluminium. The results are shown in fig-1. From the plot, we can see that there are two isochronal stages. They observed that the largest fraction of quenched-in resistivity anneals out in stage I occurring at or below room temperature. This stage I is due to the formation of dislocation loops and voids by vacancy condensation as shown by transmission microscopy[9,10] and to the annealing of vacancies to permanent sinks like dislocations and grain boundaries.

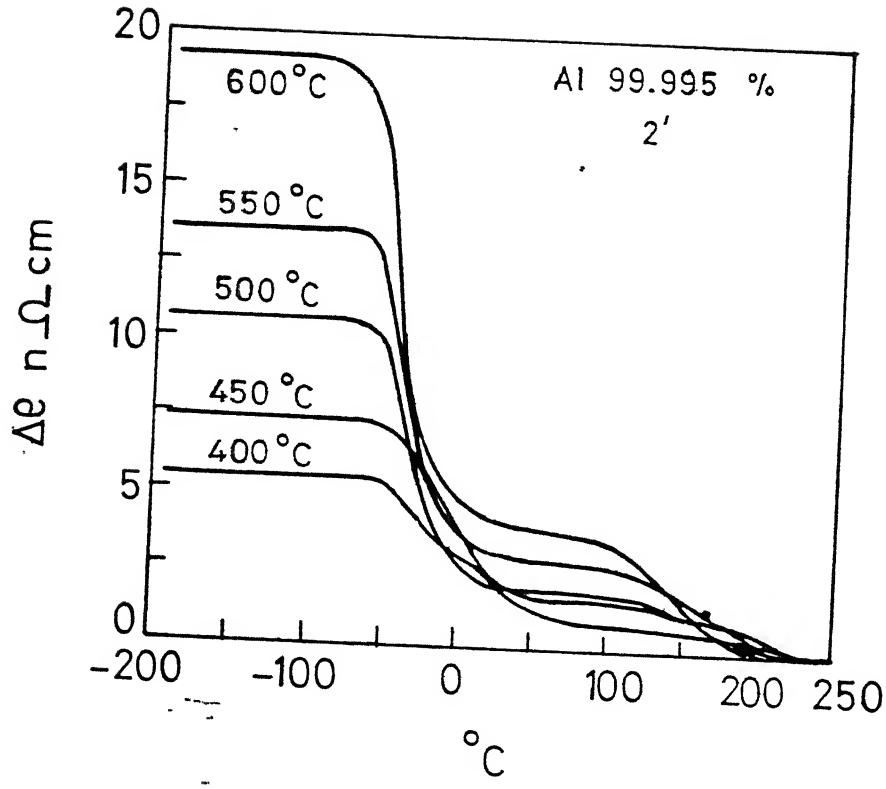

FIG.1 ISOCHRONAL ANNEALING OF PURE Al

2.4.2 Isothermal Annealing:

The simplest annealing process is one in which the defects of one species diffuse to a fixed number of unfillable sinks with no associated stress fields. In this case, the decay in concentration of defects is expected to be exponential. The rate of change of defects dn/dt is given by the relation,

$$\frac{dn}{dt} = - Kn \qquad (2.16)$$

where K is the rate constant and n is the number of defects remaining in the metal. Integrating equation (2.16)

$$n = n_o \exp(- Kt) \qquad (2.17)$$

where K, the rate constant is equal to αD and n_o is the number of defects at time zero. The constant of proportionality, α, is identified with the sink concentration.

We see that the annealing kinetics in this case are of the first order. However, several experimental results on pure aluminium[11,12] indicate the occurrence of annealing kinetics faster than the first order. This can be explained by taking divacancies into consideration. The reactions involved in this case are

$$V_1 + V_1 \underset{K_2}{\overset{K_1}{\rightleftharpoons}} V_2$$

$$V_1 \xrightarrow{K_3} \text{Sinks}$$

$$V_2 \xrightarrow{K_4} \text{Sinks} \qquad (2.18)$$

where V_1 and V_2 represent single and divacancies and K's are the rate constants. For f.c.c. metals, the rate constants can be defined by

$$K_1 = 84\nu \exp(-E_{m(1)}/kT)$$

$$K_2 = 14\nu \exp(-(E_{m(1)} + B_2)/kT)$$

$$K_3 = \alpha\nu\lambda^2 \exp(-E_{m(1)}/kT)$$

$$K_4 = \alpha\nu\lambda^2 \exp(-E_{m(2)}/kT) \qquad (2.19)$$

where $E_{m(1)}$ and $E_{m(2)}$ are the single and divacancy migration energies respectively, ν is the vibration frequency and λ is the jump distance. The rate of change of single and divacancy concentrations can be written from equation (2.18) as

$$\frac{dC_V}{dt} = 2K_2C_V - 2K_1C_V^2 - K_3C_V$$

$$\frac{dC_{2V}}{dt} = K_1C_V^2 - K_2C_{2V} - K_4C_{2V} \qquad (2.20)$$

The entire annealing process can be followed by solving equations (2.18). This has been carried out by Damask and Dienes[13] for a specific set of vacancy parameters.

In the case of impure metal or dilute alloys, every vacancy encounters a large number of impurity atoms or solutes during migration to a sink. If vacancy-impurity complex is immobile or has much lower mobility than that of free vacancy, the vacancy is trapped and the complex must dissociate before the vacancy can continue its migration towards a sink.

Damask and Dienes[14,15] have studied the annealing process by the chemical reaction approach. The following assumptions are made in this approach.

1. Vacancies form only solute-vacancy complex and no other defects i.e. avoiding the formation of divacancies, trivacancies etc.
2. Free vacancies migrate to sinks with rates equal to the annealing of vacancies in pure metal.
3. Solute-vacancy complex is immobile.

The reactions occurring can be expressed as follows,

$$V_1 + I \underset{K_6}{\overset{K_5}{\rightleftharpoons}} C$$

$$V_1 \xrightarrow{K_3} \text{Sinks} \qquad (2.21)$$

where I represents the unbound impurity atoms and C, the bound vacancies. K's are the corresponding rate constants and are defined by

$$K_5 = K_1 = 84\,\nu \exp(-E_{m(1)}/kT)$$

$$\text{and} \qquad K_6 = 7\,\nu \exp(-(E_{m(1)} + B_{Vi})/kT) \tag{2.22}$$

The differential equations for these reactions can be written (after substitution $I = I_o - C$) as

$$\frac{dC}{dt} = K_1 I_o C_V - K_1 C_V C - K_2 C \tag{2.23}$$

$$\frac{dC_V}{dt} = - K_1 I_o C_V + K_1 C C_V + K_2 C - K_3 C_V \tag{2.24}$$

where I_o is the total impurity concentration, which is a constant for any given experiment. The total vacancy concentration ($N = C + C_V$) is described by the differential equation

$$\frac{dN}{dt} = \frac{d(C + C_V)}{dt} = \frac{dC}{dt} + \frac{dC_V}{dt} = - K_3 C_V \tag{2.25}$$

Equations (2.23) and (2.24) form a set of non linear coupled differential equations which, when solved, will describe the complete annealing behaviour of the system. The equilibrium concentration of vacancies at the annealing temperature is negligibly small, and hence C_V and C approach zero as time approaches infinity.

The computer solution of these equations shows that the number of complexes, C, increases very rapidly during the early stages of annealing. During the same transient period the concentration of free vacancies decreases rapidly. After these fast transients, C and C_V decay slowly. These fast transients will result in the establishment of equilibrium between C_V and C, characteristic of the annealing temperature. The rapid elimination of these transient conditions suggests that an analytical approximation can be used for the bulk of the vacancy decay curve. Equilibrium for the reaction represented by the equation (2.21) implies that

$$\frac{C}{C_V(I_o - C)} = \frac{K_5}{K_6} \qquad (2.26)$$

which is also the condition for steady-state approximation on C, i.e., $\frac{dC}{dt} = 0$. A further approximation, namely, $C \ll I_o$ leads to

$$\frac{C}{C_V} = I_o \frac{K_5}{K_6} \qquad (2.27)$$

substitution of equation (2.27) in equation (2.25) and integration gives,

$$C + C_V = N = C'_{V(o)} \left[1 + (I_o K_5/K_6)\right] \exp(- K_e t) \qquad (2.28)$$

where $C'_{V(o)}$ is the free vacancy concentration at the beginning of exponential decay and,

$$K_e = \frac{K_3}{(1 + I_o K_5/K_6)} \tag{2.29}$$

K_5/K_6 is defined by

$$\frac{K_5}{K_6} = 12 \exp\left(\frac{B_{Vi}}{kT}\right)$$

The equation (2.29) can now be rewritten as,

$$K_e = \frac{K_3}{1 + 12\ I_o \exp(B_{Vi}/kT)} \tag{2.30}$$

K_3 can be determined by carrying out an isothermal annealing experiment on a pure sample and K_e can be found out by a similar experiment on an alloy at the same temperature, B_{Vi} can be found out by using the equation (2.30). It can also be noted that

$$N = N_o \exp - K_e t \tag{2.31}$$

where N_o is the total vacancy concentration at zero time.

Damask and Dienes, in their analysis assume that vacancy concentration is sufficiently low so that higher order complexes like divacancies are absent. However, when quenching temperatures are higher, divacancies are formed. There will be simultaneous annealing of single and divacancies. The corresponding kinetic scheme is

$$V_1 + I \underset{K_6}{\overset{K_5}{\rightleftharpoons}} C$$

$$V_1 + V_1 \underset{K_2}{\overset{K_1}{\rightleftharpoons}} V_2$$

$$V_1 \xrightarrow{K_3} \text{Sinks}$$

$$V_2 \xrightarrow{K_4} \text{Sinks}$$

The differential equations for these reactions can be written after substitution $I = I_o - C$ as

$$\frac{dC_V}{dt} = - K_1 C_V I_o + K_1 C_V C + K_2 C - K_4 C_V^2 + K_5 C_{2V} - K_3 C_V$$

$$\frac{dC_{2V}}{dt} = \frac{1}{2} K_4 C_V^2 - \frac{1}{2} K_5 C_{2V} - K_6 C_{2V}$$

$$\frac{dC}{dt} = K_1 C_V I_o - K_1 C_V C - K_2 C \qquad (2.32)$$

Since the total vacancy concentration $N = C_V + 2C_{2V} + C$,

$$\frac{dN}{dt} = \frac{dC_V}{dt} + \frac{2dC_{2V}}{dt} + \frac{dC}{dt} = - K_3 C_V - 2K_6 C_{2V} \qquad (2.33)$$

Chik[16] has solved, the equation (2.33) using the steady state approximation on divacancies i.e. $dC_{2V}/dt = 0$. Lahiri[17] et al, Singh[18] have solved these equations in a computer using known values for $E_{m(1)}$ and

$E_{m(2)}$ to arrive at the variation of C_V, C_{2V} and N as a function of time. As in the case of single vacancy annealing in alloys, there are initial transients followed by a steady decay. The transients correspond to the reestablishment of equilibrium between C_V, C_{2V} and C, characteristic of the temperature of annealing.

2.5 DETERMINATION OF BINDING ENERGY FROM ELECTRICAL RESISTIVITY MEASUREMENTS:

Electrical resistivity measurements are commonly used for the determination of E_V^f, B_2 and B_{Vi}. The principle of this technique is based on the Mattheiessen's rule, which states that the total resistivity of the material (ρ) is equal to the sum of the contributions from lattice vibration (ρ_T) and defects (ρ_D), i.e.

$$\rho = \rho_T + \rho_D \tag{2.34}$$

If in an experiment the concentration of all defects excepting point defects is kept constant, the value of ρ varies slightly depending on the point defect concentration

$$\rho = \rho_T + \rho_D' + \rho_{P.D.} \tag{2.35}$$

where $\rho_{P.D}$ is the resistivity contribution due to point defects and ρ_D' that due to all other defects.

The sum of ρ_T and ρ'_D can be obtained by making measurements on a well annealed sample (ρ_a). If this is compared with the resistivity of a quenched sample (ρ_q), there is a small difference, $\Delta\rho$, equal to,

$$\Delta\rho = A' \exp(-E_V^f/kT_q) \tag{2.36}$$

where A' is constant.

If a set of several quenching temperatures is used then a plot of $\ln\Delta\rho$ against $1/T_q$ is linear with slope equal to $-E_V^f/K$.

In order to avoid complications due to divacancies, it is necessary to use low quenching temperatures. When a similar experiment is carried out on an alloy, the extra resistivity alloy can be defined as,

$$\Delta\rho_{alloy} = A'' \exp(-E_V^f/kT_q)\left(1 - \overline{Z+1} + ZI_o\epsilon \exp\frac{B_{Vi}}{kT_q}\right) \tag{2.37}$$

where A" is a constant and ϵ is the contribution of a bound vacancy to electrical resistivity. A plot of $\ln\Delta\rho_{alloy}$ against $1/T_q$ over narrow temperature ranges is usually linear with the slope given by $-E_V^{f*}/k$ where E_V^{f*} is the apparent energy of formation of vacancy in the alloy.

From equation (2.37), it is clear that

$$E_V^f - E_V^{f*} = \frac{\left[Z B_{Vi} I_o \exp(B_{Vi}/kT_q) \right]}{\left[1 - (Z+1)I_o + \epsilon Z I_o \exp(B_{Vi}/kT_q) \right]} \qquad (2.38)$$

By considering clustering during quenching, Lahiri et al[19] have shown that,

$$E_V^f - E_V^{f*} = \frac{\left[ZI_o B_{Vi} \exp(B_{Vi}/kT_q) \right]}{\left[1 - (Z+1)I_o + ZI_o \exp(B_{Vi}/kT_q) \right]} \qquad (2.39)$$

So knowing E_V^f, E_V^{f*}, I_o and T_q, B_{Vi} can be calculated.

A second method of calculating the binding energy of the solute-vacancy complex involves quenching the pure metal and the alloy from the same temperature and measuring the extra resistivities $\Delta\rho$ and $\Delta\rho_{alloy}$. The two are related by the expression

$$\frac{\Delta\rho_{alloy}}{\Delta\rho} = 1 - 13I_o + 12I_o \exp(B_{Vi}/kT_q) \qquad (2.40)$$

A plot of $\Delta\rho_{alloy}/\Delta\rho$ against $1/T_q$ is linear with slope equal to B_{Vi}/k.

The migration energy of a vacancy can be calculated by carrying out isothermal annealing studies on a quenched metal. From equation (2.17),

$$\Delta\rho_t = \Delta\rho_o \exp(-Kt) \qquad (2.41)$$

where $\Delta\rho_o$ and $\Delta\rho_t$ are the extra resistivities at zero time and time t respectively. A plot $\ln(\Delta\rho_t/\Delta\rho_o)$ against t is linear with slope equal to (-K). A plot of ln K against 1/T (the data obtained from several isothermal annealing experiments) is linear with slope of $-E_{m(1)}/K$. Obviously, in order to minimise complications due to divacancies, low quenching temperatures are to be used.

When a similar experiment is performed on an alloy, the plot of $\ln(\Delta\rho_{t(alloy)}/\Delta\rho_{o(alloy)})$ against time leads to an estimate of K_e. From equation (2.29), once K_3 is known from annealing data of a pure metal, the ratio of K_5/K_6 can be calculated. This ratio is equal to $12\exp(B_{Vi}/kT)$. Hence B_{Vi} can be determined by comparing the annealing curves of a pure metal and its alloy.

2.6 DIFFUSION IN ALUMINIUM-TRANSITION-METAL ALLOY:

The activation energies for the diffusion of transition metals in aluminium are found to be anomalously high (Table 1)[3].

The precipitation of Mn and Cr from super saturated aluminium alloy is sluggish even at temperature of 350°C.[17,20] On the basis of these considerations it is expected that the binding energy of the elements

TABLE I – Experimental values of activation energies for diffusion of 3d transition solutes in Al

Solute	Activation energy in eV
Cr	2.64
Mn	2.19
Fe	2.48
Co	1.81
Ni	1.31
Cu	1.40

would be high. The kinetic measurements made on Al - 0.1 wt % Mn and Al - 0.35 wt % Mn alloys[17,18] have shown that the manganese-vacancy binding energy is of the order of 0.1 eV. This value is lower than that quoted for a number of elements like Cd, In and Sn. In this investigation the kinetics of annealing of vacancies in Al - 0.1 wt % Cr alloy has been studied.

2.7 ALUMINIUM-CHROMIUM SYSTEM:

There is a peritectic reaction in the aluminium-chromium system at a temperature 661.4 ± 0.1°C,[21] at which point maximum solid solubility of chromium in aluminium is 0.72 wt % (0.375 at.%). The solid phases

present at peritectic temperature are α-solid solution phase and θ, which is an intermediate phase having formula $CrAl_7$. The solid solubility limits of chromium in aluminium have been reported in table 2.[22]

TABLE 2

Temperature °C	Solubility limit of chromium wt %
630	0.58
600	0.45
550	0.30
500	0.19
400	0.06
300	0.015

It has been seen that chromium has comparatively low solid solubility in aluminium which decreases very rapidly with fall in temperature.

CHAPTER 3

EXPERIMENTAL TECHNIQUES

3.1 MATERIALS REQUIRED:

The present investigation has been carried out on the following materials:

(i) Pure aluminium, 99.999% pure

(ii) Aluminium - 0.1 wt % Chromium.

The Al - 0.1 wt % Cr has been prepared from 99.999% pure Al and 99.99% pure Cr.

3.2 PREPARATION OF ALLOY:

The pure aluminium rod has been cut into small slices. The slices have been cleaned in dilute NaOH solution and than washed with water several times and finally with acetone. The chips of chromium have been immersed in dilute hydrochloric acid solution for about ten minutes and then washed with water and alcohol. The necessary amounts of pure metals have been taken in a quartz tube which has been sealed in vacuum and introduced in a globar furnace maintained at 1200°C. Sufficient time (about 8 hours) has been allowed at this temperature in order to ensure complete

homogenisation of the molten alloy. The quartz tube has then been removed from the furnace and cooled. The solid alloy has been removed by breaking the quartz tube and homogenised at 600°C for 120 hours.

The homogenised Al - 0.1 wt % Cr alloy has been swaged in a number of stages until its diameter has been reduced to 2.5 mm. Intermediate annealing treatments at 500°C for 4 hours have been given in between every swaging treatment to prevent cracking the rod during swaging. The annealed 2.5 mm diameter wire has been drawn through a wire drawing dic in a number of stages to the final diameter of about 1 mm. After every stage, care has been taken to avoid contamination by cleaning the wire with NaOH solution. Chemical analysis of the sample has shown that it contained 0.095 wt % Cr with traces $<$ 0.001 wt % of Cu and Mg.

3.3 SAMPLE PREPARATION:

The wire of pure Al or alloy of 60 cm length has been wound on a glass rod having an outer diameter of 7 mm in the form of helical coil leaving 4 cm long straight wire at each end. As we will see in the subsequent section, the resistance measurements require separate potential and current leads. Four separate wires each of 70 cm length of the same metal or alloy and of same size as the specimen

have been taken, two of them, have been fused to each end of the sample. The following flux has been used for the fusing of the wires,

Potassium chloride	26% by wt.
Lithium chloride	27% by wt.
Sodium chloride	32% by wt.
Sodium fluoride	15% by wt.

The method adopted has been the same as that described by Lahiri[17].

3.3.1 Sample Assembly:

After the sample has been made as described in the previous section, it has become necessary to have some means for easy handling of them and quick recognition of potential and current leads; also the current and potential leads should not come in live contact with one another. In order to avoid these difficulties, all the four leads wire have been insulated with the help of porcelain beads to a length of 40 cm from the junction of the lead wire and the specimen. For easy identification of the current and potential leads, different types of porcelain beads have been placed on each lead wire and they have been numbered as 1, 2, 3 and 4. This has facilitated quick and correct connection of the sample to the resistance measuring device. The sample has been tied with the help of a pure

aluminium wire on to a stainless steel rod of about 2.5 mm diameter and 45 cm long, to facilitate rapid quenching of the sample. While tightening potential and current leads with pure aluminium wire, care has been taken that the aluminium wire has not been touching the lead wires. While measuring the electrical resistance the problem of short-circuiting of the lead wire has been avoided by inserting them into a four-holed neoprene sheet. This sample assembly has been found suitable for resistance measurement; it is shown schematically in fig. 2.

3.4 ELECTRICAL RESISTANCE MEASURING UNIT:

The electrical resistivity of the sample is given by the following relation,

$$\rho = R/(l/A) \qquad (3.1)$$

where R = Resistance of the sample in ohms

l = Length of the sample in cms

A = Cross-sectional area of the sample in cm^2

and ρ = Resistivity of the material of the sample in ohm-cm.

The length of the sample and the cross-sectional area are chosen as a compromise between precise measurement of

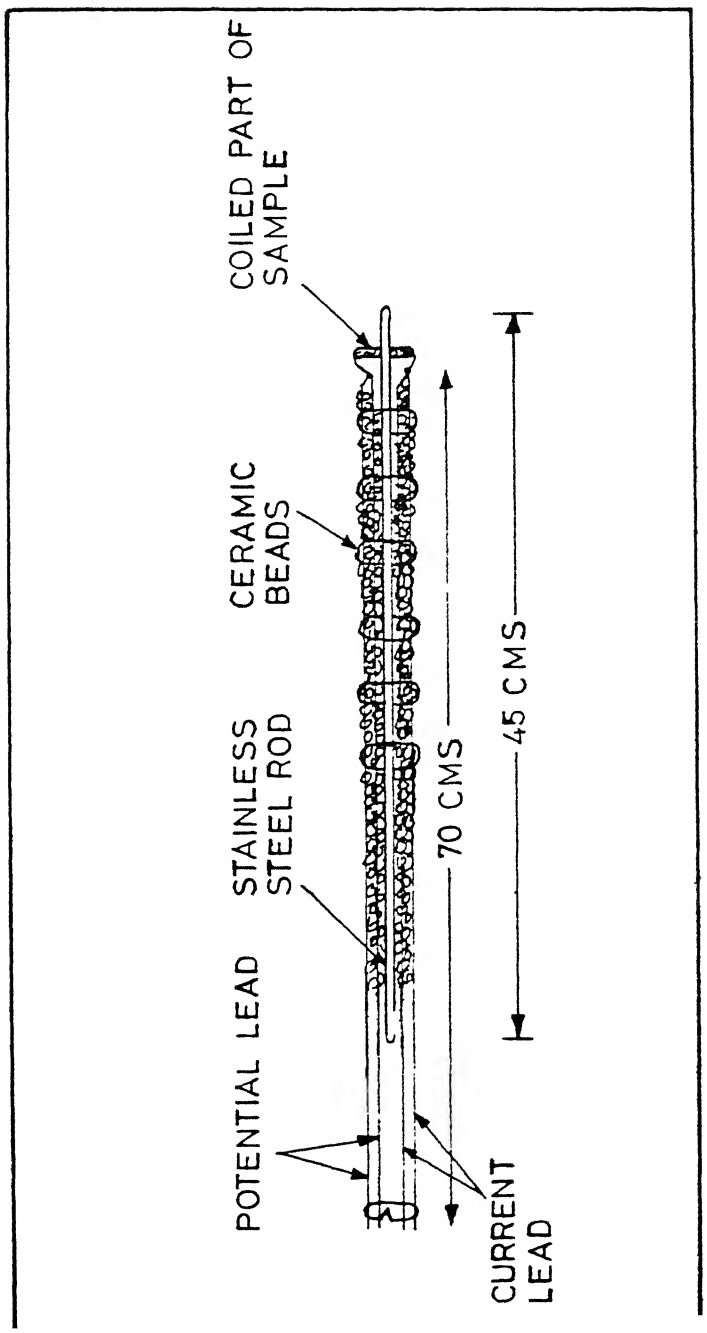

FIG. 2 SAMPLE ASSEMBLY

resistivity and the maximum resistance that can be measured on the Precision Kelvin bridge. In the present investigation the variation in the resistivity of the sample as a function of different treatments has been measured. The relevant relation for this case is,

$$\Delta\rho = \frac{\Delta R}{(l/A)} \qquad (3.2)$$

where ΔR and $\Delta\rho$ are the change in resistance and resistivity respectively. The ratio (l/A) will remain constant for one sample; thus equation (3.2) reveals that change in resistivity, $\Delta\rho$, will be directly proportional to the change in resistance, ΔR. The length-to area ratios of the samples used in the present investigation are shown in Table 3.

TABLE 3

(l/A) Ratio of Samples for Resistance Measurement

Material used	Sample No.	Diameter of wire mm	Length of sample cms	(l/A) cm^{-1}
Al 99.999% Al	1	0.808	59.2	11.540×10^{3}
	2	0.840	59.0	10.642×10^{3}
Al - 0.095 wt % Cr alloy	1	0.998	56.9	7.268×10^{3}
	2	0.998	58.4	7.466×10^{3}

3.4.1 Precision Kelvin Bridge:

The precision Kelvin bridge is a general purpose Kelvin bridge for making low resistance measurements essentially independent of lead and contact resistance. It is used to measure the resistance of precision resistors, of wires, rods and bars. The Kelvin bridge method requires separate potential and current leads. The unknown and the standard resistances are connected to the bridge as shown in Fig. 3. The various elements of the circuit are identified below:

X is the resistance to be measured between points p and p'.

R is the standard resistance for comparison with X. The potential points t and t' are movable to vary the resistance between them.

A and B are the calibrated resistances in the main ratio arms of the bridge circuit

a and b are the calibrated resistances in the auxiliary ratio arms.

d is the connection, called yoke, between one end of X and the adjacent end of R.

m, n, Z and Y are the resistances of leads and contacts in connections between the ratio arms and the two conductors.

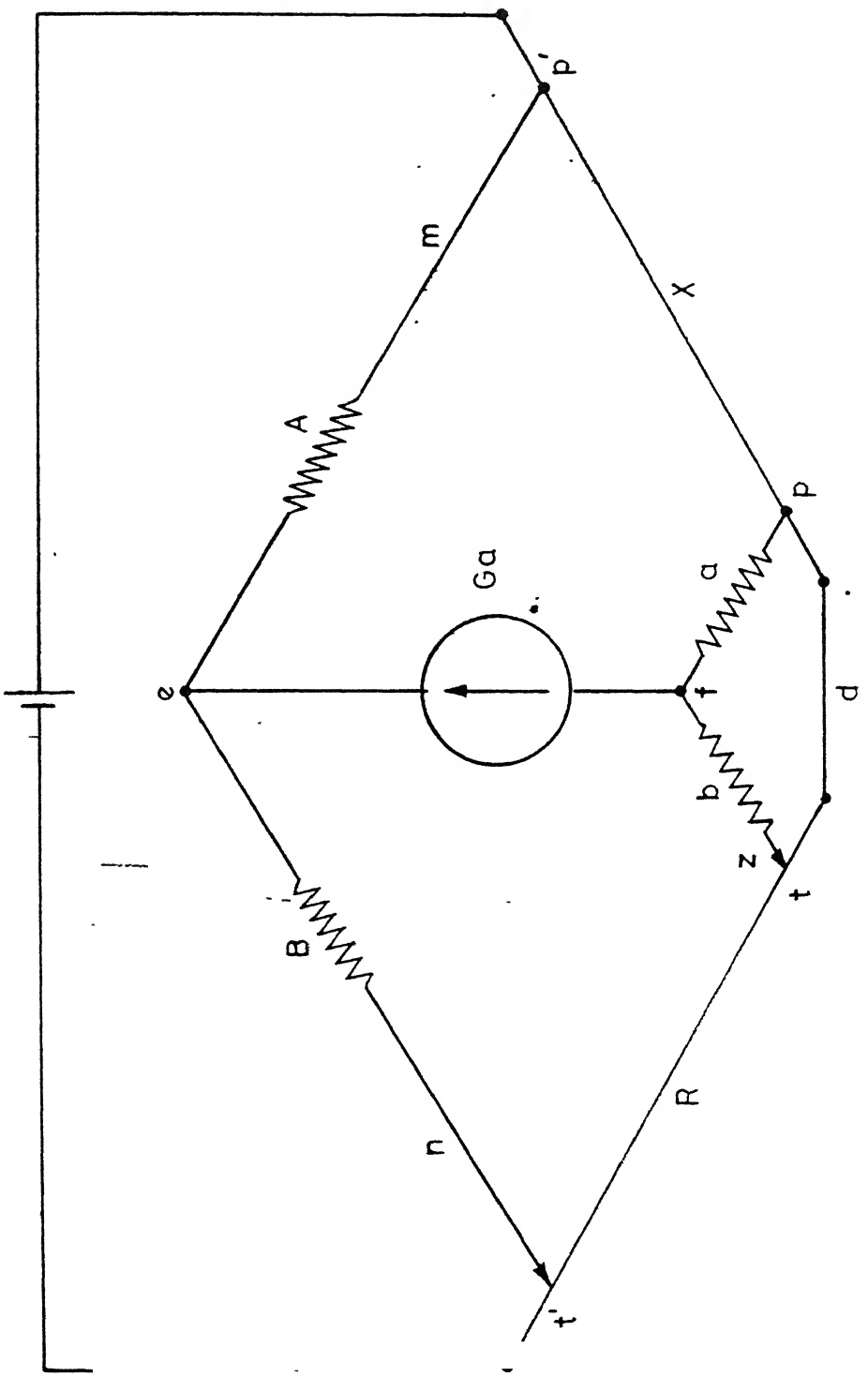

FIG. 3 DIAGRAM OF KELVIN BRIDGE CIRCUT

When the elements of the circuit are adjusted so that no current flows in the galvanometer, the resistance X between the points p and p' is related to the resistance R between the points t and t' as the resistance A is related to the resistance B. Hence, the working relation for Kelvin bridge under balanced condition is,

$$\frac{X}{R} = \frac{A}{B} = \frac{a}{b} \qquad (3.3)$$

The operation of Kelvin bridge is discussed in detail in the literature[23-25]. The interconnection diagram of the precision Kelvin bridge is shown in Fig. 4.

3.5 EXPERIMENTAL SET-UP:

The various units used and the detailed procedure for carrying out measurements are given in the following sections.

3.5.1 Annealing Furnace (High Temperature Furnace):

This is a vertical tube electrical furnace. The furnace is fitted with mullite tube 390 mm long and 50 mm internal diameter. The bottom of the furnace has been sealed. The furnace has been calibrated for maximum temperature zone. It has been found that the constant temperature zone is just about 25 mm above the sealing plug.

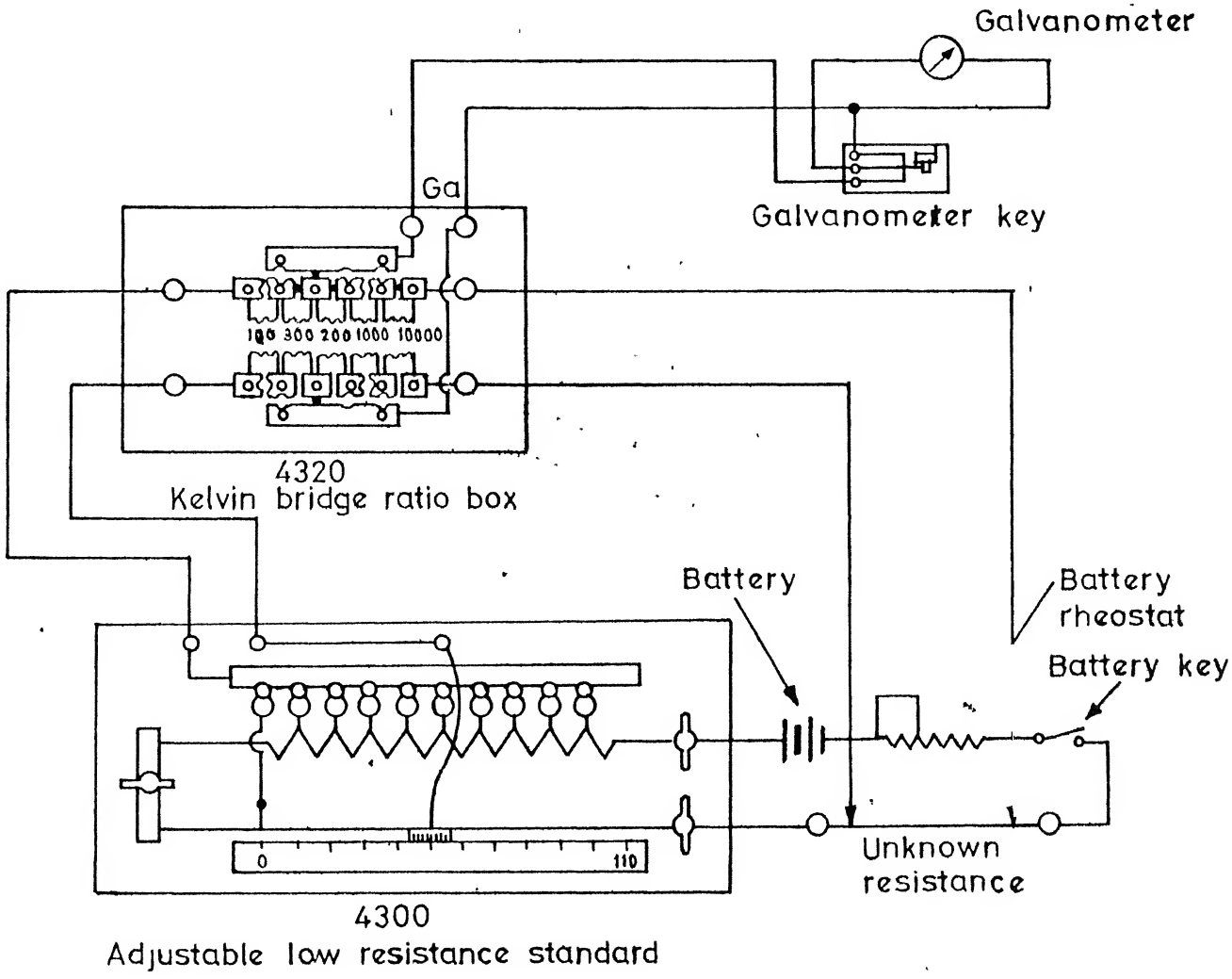

FIG. 4 INTERCONNECTION DIAGRAM PRECISION KELVIN BRIDGE

The furnace has been closed from top with the help of a refractory lid. This lid has been sliced into two vertical halves. In one half, two holes have been made to insert chromel-alumel thermocouples. A small circular groove has been made in the centre of the two vertical halves of the refractory lid in order to keep the sample in the furnace. One thermocouple has been connected to the potentiometer to measure the accurate furnace temperature.

3.5.2 Quenching Furnace:

This furnace has been similar to that of the annealing furnace excepting that the bottom has been kept open. It has a tube of internal diameter 70 mm and length 460 mm. This furnace has been kept on a raised platform. This platform has a big hole of about 100 mm at centre which has been fitted with a metallic plate, hinged to the platform to close and open the opening in the platform. Similarly furnace has been closed at the top by two vertical halves of refractory. One half of it, is fitted with two thermocouples and this lid has been tightened with wire. With the help of other half of refractory lid, the sample has been kept in the furnace for quenching. One thermocouple has been connected to a potentiometer for accurate temperature measurement and the other to a L and N temperature controller.

3.5.3 Quenching Vessel:

A steel pipe 100 cm long and 10 cm internal diameter with its bottom closed has been mounted vertically on a four wheeled trolley to facilitate the movement of the quenching vessel. The pipe is wrapped with asbestos cloth. A thermocole spongy packing was tightly inserted to a depth 72 cm from the top of the pipe. The total height of this assembly has been adjusted so that the top end of the pipe is below the bottom end of the quenching furnace.

3.5.4 Constant Temperature Bath:

For working upto a temperature of 80°C, a constant temperature bath has been made by taking a one litre capacity beaker filled with water and placing it in a 3 litre capacity cylindrical Dewar flask such that the top periphery of beaker has been at the same level as that of the flask. The temperature of the bath has been controlled with the help of a 250 watts water heater along with a Fischer proportional controller[26]. An electric stirrer has been used for stirring the bath.

3.5.5 High Temperature Bath:

For working in the temperature range 80°C to 260°C, an oil bath has been used. The oil used for this purpose is DM silicone fluid. A two litre glass beaker

has been covered on the sides with a soft asbestos sheet over which a thick asbestos rope has been wound. The beaker has been filled with DM silicone fluid and then placed in a heating mantle. The actual temperature of the oil bath has been measured by a thermometer of graduations 0.1°C, inserted from the top.

3.6 RESISTANCE MEASURING BATH:

The resistance of the sample has been measured at the boiling point of liquid nitrogen (78°K). The reasons for using liquid nitrogen can be summarised as follows:

a) The quenched-in vacancies can be retained at sufficiently low temperature without any loss, and

b) The total resistivity of the sample decreases sharply with decrease in temperature. Since the resistivity contribution due to quenched-in vacancies is a small fraction of the total resistivity of the sample, the resistivity due to quenched-in vacancies is measured better at a low temperature.

3.7 EXPERIMENTAL PROCEDURE:

The sample has been soaked for 30 minutes at a temperature of 500°C in the quenching furnace. The sample

has been quenched from this furnace into brine solution maintained at about 1°C in the quenching vessel. After quenching, the sample has been transferred into a Dewar flask filled with liquid nitrogen through ice cooled acetone. This whole operation from opening of the lid of the quenching furnace to the transfer of the sample assembly to the Dewar flask having liquid nitrogen has taken less than 4-5 seconds. Care has been taken that the level of liquid nitrogen has been at least 40 mm above the junction of the leads.

3.8 ISOCHRONAL ANNEALING EXPERIMENT:

Isochronal annealing has been carried out for both the pure aluminium as well as the Al - 0.095 wt % Cr alloy samples. In this experiment, the sample has been annealed for 30 minutes at 500°C, as described in Section 3.7. The as-quenched resistance has been measured at liquid nitrogen temperature, the sample has been progressively annealed at temperatures starting from 0 to 260°C for a fixed time of 5 minutes at each temperature. After each annealing, the resistance has been measured at liquid nitrogen temperature. For annealing upto 80°C, water bath has been used, whereas, for temperatures from 100°C onwards DM silicone fluid bath has been used.

3.9 ISOTHERMAL ANNEALING AT LOW TEMPERATURES:

Isochronal annealing experiments on the pure metal and the alloy samples reveal that there is a recovery stage occurring around 20°C. To characterise this recovery stage isothermal annealing experiments have been made at 0, 10, 20 and 30°C. The procedure is similar to that described in Sections 3.7 and 3.8. After measuring the as-quenched resistance at liquid nitrogen temperature, the sample assembly has been transferred to the constant low temperature bath for annealing at constant temperature via ice cooled acetone. After known interval of time, the sample has been transferred to the Dewar flask having liquid nitrogen via. ice cooled acetone and the resistance measured. The process has been repeated for different time periods of annealing and finally the sample has been annealed at 70°C for 30 minutes in a water bath and the resistance has been again measured. The isochronal curves (see next chapter) indicate that the first stage is complete by about 50°C, therefore the 70°C anneal should ensure that the material has been taken beyond this stage.

3.10 ISOTHERMAL ANNEALING AT HIGH TEMPERATURE:

Isothermal annealing has been carried out on the Al - 0.095 wt % Cr alloy, at 250°C, to see whether any precipitation occurs. The quenched resistance has been measured after soaking the sample for 30 minutes at 500°C as described in Sections 3.7 and 3.8. The isothermal annealing has been carried out in the DM silicone fluid bath. The sample has been kept in the silicone fluid bath for a known interval of time and then transferred into Dewar flask having liquid nitrogen via ice cooled acetone and the resistance has been measured. This process has been repeated till the completion of the precipitation reaction as indicated by constancy in the resistance value. The change in resistance, ΔR, at a particular annealing time 't' is given by

$$\Delta R = R_q - R_t$$

or

$$\Delta \rho = \rho_q - \rho_t \qquad (3.4)$$

where $\Delta \rho$ = excess resistivity

ρ_q = as quenched resistivity

and ρ_t = resistivity at time 't'.

CHAPTER IV

RESULTS AND DISCUSSION

4.1 INTRODUCTION:

As pointed out in Chapter 1, the present investigation has been concerned with the study of chromium-vacancy binding energy in aluminium. There are three different steps involved in this study, viz.

i) study of isochronal annealing of pure aluminium and aluminium-chromium alloy quenched from a suitable temperature,

ii) after the identification of the recovery stages from the isochronal annealing curve, carrying out isothermal annealing at a suitable temperature range, and

iii) to calculate the chromium-vacancy binding energy from the isothermal annealing data of pure aluminium and aluminium-chromium alloy.

The technique of electrical resistivity measurement has been used for the studies and all the measurements have been made at liquid nitrogen temperature (78°K). It has been found by trial and error that the quench temperature of 500°C has been suitable for the

studies. From the excess resistivity obtained by quenching from this temperature, it has been possible to make a number of measurements for the decay in resistivity as a function of time or temperature.

4.2 RESISTIVITY OF PURE ALUMINIUM AND ALUMINIUM - 0.095 wt % CHROMIUM ALLOY:

The resisitivities of aluminium 99.999% pure and aluminium-chromium alloy have been measured at liquid nitrogen temperature (78°K). In this case the samples have been soaked at the temperature 500°C and quenched in brine solution maintained at 1°C and the resistivities have been measured after quickly transferring the sample to the liquid nitrogen bath. This experiment has been repeated three times in the case of pure aluminium; in the case of alloy the experiment has been repeated four times. The results have been tabulated in table 4.

TABLE 4

Resistivities of Al and Al-Cr alloy

Quenching temperature = 500°C

Material	Resistivity at 78°K in micro-ohm cm				
	EXPERIMENT NO.				Mean value
	I	II	III	IV	
99.999% Al	0.2285	0.2288	0.2286	-	0.2286± 0.0002
Al-0.095 wt%Cr	0.6531	0.6523	0.6529	0.6525	0.6527±0.0004

The mean value of 0.2286±0.0002 micro-ohm cm obtained for pure aluminium agrees well with the value 0.24 micro-ohm cm obtained by Lahiri[17] on 99.999% pure aluminium and 0.23 micro-ohm cm obtained by Panseri and Federighi[8] on 99.995% pure aluminium.

The resistivity of aluminium-chromium (0.049 at %) alloy is 0.6527±0.0004 micro-ohm cm. Since this is a quenched alloy, all the chromium will be in solid solution and therefore the contribution to resistivity of chromium in aluminium is 8.66 micro-ohm cm/at %. This value compares well with that of 8.3 micro-ohm cm per at % of chromium obtained by Kedves et al[27]

4.3 ISOCHRONAL ANNEALING OF PURE ALUMINIUM AND ALUMINIUM-0.095 wt % CHROMIUM ALLOY:

The results of isochronal annealing of pure Al and Al - 0.095 wt % Cr alloy have been tabulated in tables 5 and 6 respectively and plotted in Figures 5 and 6 respectively. $\Delta\rho$, the excess resistivity is defined by the relation

$$\Delta\rho = \rho_q - \rho_t \qquad (4.1)$$

TABLE 5

Isochronal annealing of pure aluminium

Quenching temperature = 500°C

Annealing time = 5 minutes at each temperature

Annealing Temp. °C	$\Delta \epsilon$ n-ohm cm
-195	0.0
0	1.2
10	2.0
20	2.7
30	3.3
40	3.7
50	4.3
60	4.4
70	4.5
80	4.7
100	4.9
120	4.9
140	5.0
160	5.1
180	5.5
200	6.3
220	6.9

TABLE 6

Isochronal annealing of Al - 0.095 wt % Cr alloy

Quenching temperature = 500°C

Annealing time = 5 minutes at each temperature

Annealing Temp. °C	$\Delta\rho$ n-ohm cm
195	0.0
0	1.4
10	2.4
20	3.3
30	3.8
40	4.3
50	4.3
60	4.3
70	4.3
80	4.5
100	5.0
120	5.1
140	5.4
160	5.7
180	6.0
200	6.0
220	6.8
240	7.4

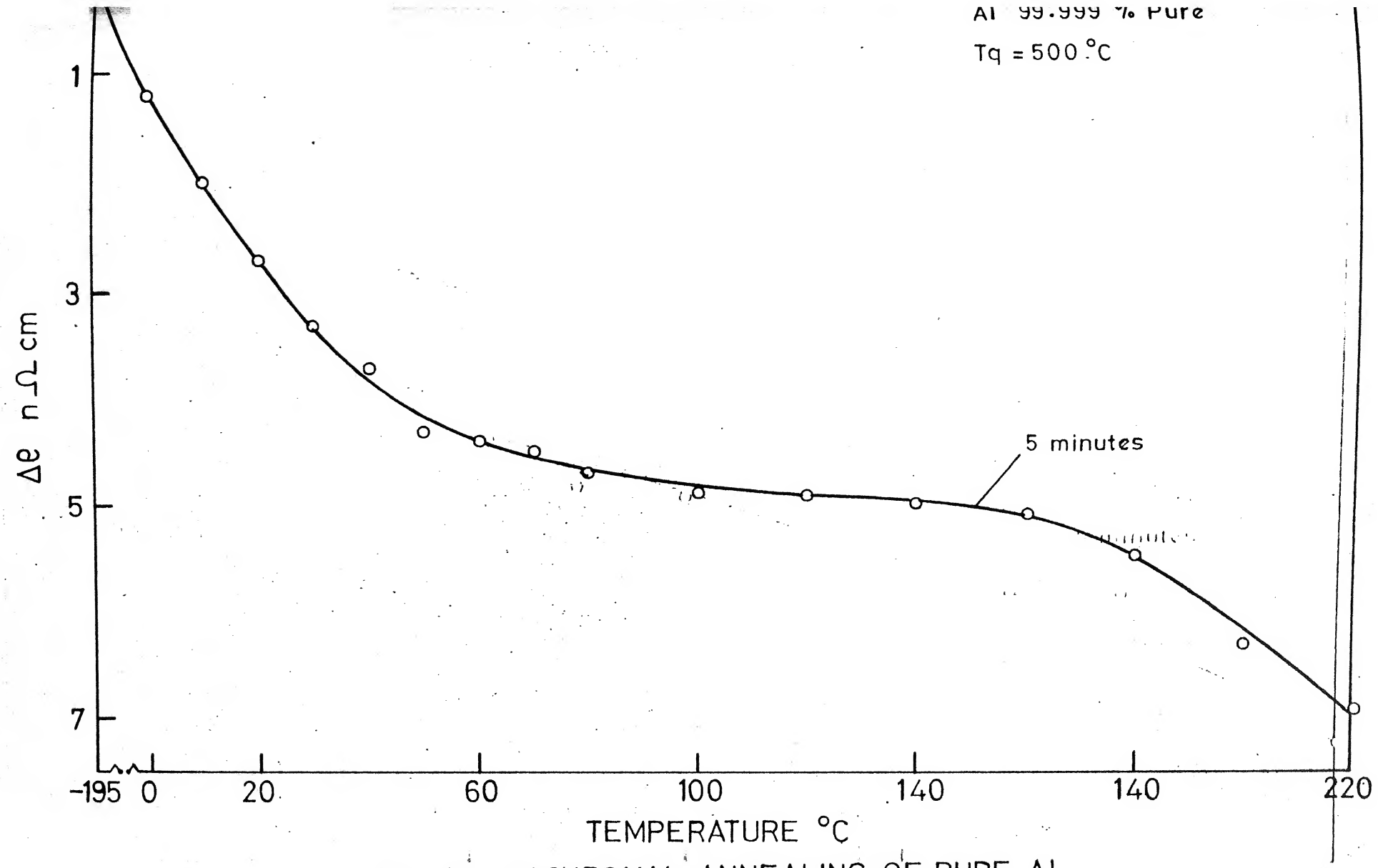

FIG. 5 ISOCHRONAL ANNEALING OF PURE Al

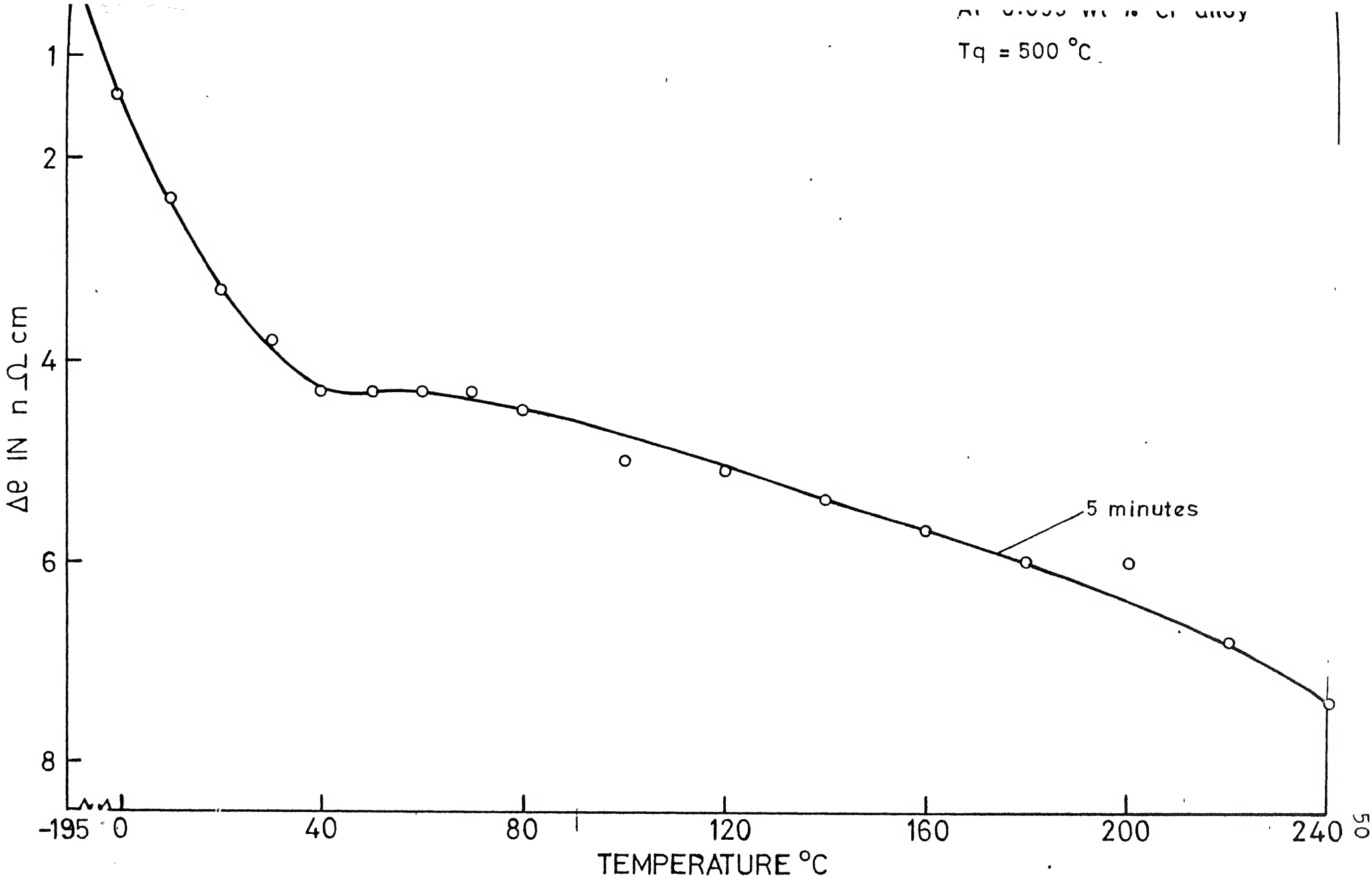

FIG.6 ISOCHRONAL ANNEALING OF QUENCHED Al-0.095 Wt % Cr ALLOY

where ρ_q is the as quenched resistivity and ρ_t is the resistivity after annealing for time t.

The time of annealing for each temperature has been 5 minutes. The experiment for pure aluminium has been repeated 3 times whereas that for the alloy 4 times. The mean values have been reported in the tables 5 and 6.

A close look at Figure 5, shows that there are two recovery stages — stage I is in the temperature interval 0 to 50°C and the second stage between 140-220°C. The two recovery stages obtained are similar to those observed by Federighi[2] (Refer to Figure 1, Chapter 2). Similarly in the quenched Al-Cr alloy too there are two stages — stage I in the temperature range 0 to 40°C and the stage second between temperature range 120 to 240°C.

A comparison of Figures 5 and 6 indicates that the two stages occurring in pure aluminium and the alloy are similar and it is difficult to draw any conclusions regarding the addition of chromium on the isochronal annealing behaviour of quenched aluminium.

The first recovery stage in pure aluminium is associated with the annealing of excess vacancies to permanent sinks such as grain boundaries and dislocations and also with the formation of dislocation loops and

voids[2]. The second stage in pure aluminium is associated with the shrinkage of dislocation loops[2,9]. In the alloy, the first stage should be associated with the annealing of vacancies to permanent sinks and in the formation of the dislocation loops. The absence of any resistivity peak in the alloy in this stage is perhaps an indication of the absence of clustering. Stage II in the alloy can be associated both with the shrinkage of dislocation loops and with the possible precipitation of chromium from super saturated solid solution. Isothermal annealing studies on the decomposition of the super saturated solid solution (see Section 4.5) suggests that precipitation occurs at about 250°C.

4.4 ISOTHERMAL ANNEALING OF PURE ALUMINIUM AND ALUMINIUM - 0.095 wt % CHROMIUM ALLOY:

Several isothermal annealing experiments have been carried out in the temperature range 0 to 30°C on pure aluminium and the aluminium-chromium alloy. The experiment has been repeated at least three times at each temperature. The results have been tabulated in tables 7 to 14 and plotted in the Figures 7 to 12. For the annealing experiments, the following relations have been used,

TABLE 7

Isothermal annealing of 99.999% aluminium

Quenching temperature = 500°C

Annealing temperature = 0°C

Annealing Time Minutes	$(\frac{\Delta\epsilon}{\Delta\epsilon_o})$	$\log(\frac{\Delta\epsilon}{\Delta\epsilon_o})$	$(\frac{\Delta\epsilon_o}{\Delta\epsilon} - 1)$
0	1.0000	0.0000	0.0000
2	0.9382 ± 0.0036	-0.0277	0.0659
4	0.8842 ± 0.0131	-0.0534	0.1310
6	0.8354 ± 0.0098	-0.0781	0.1970
8	0.7877 ± 0.0052	-0.1036	0.2695
10	0.7464 ± 0.0335	-0.1270	0.3398
12	0.7052 ± 0.0342	-0.1517	0.4180
14	0.6712 ± 0.0206	-0.1732	0.4899
16	0.6576 ± 0.0372	-0.1820	0.5207
18	0.6299 ± 0.0502	-0.2007	0.5876
20	0.6230 ± 0.0358	-0.2055	0.6051
22	0.5883 ± 0.0432	-0.2304	0.6998
24	0.5609 ± 0.0456	-0.2511	0.7828
26	0.5472 ± 0.0451	-0.2618	0.8275
28	0.5126 ± 0.0581	-0.2802	0.9508

TABLE 8

Isothermal annealing of Al - 0.095 wt % Cr alloy

Quenching temperature = 500°C

Annealing temperature = 0°C

Annealing Time Minutes	$(\frac{\Delta\epsilon}{\Delta\epsilon_0})$	$\log(\frac{\Delta\epsilon}{\Delta\epsilon_0})$	$(\frac{\Delta\epsilon_0}{\Delta\epsilon} - 1)$
0	1.0000	0.0000	0.0000
2	0.9022 ± 0.0250	-0.0447	0.1084
4	0.8456 ± 0.0500	-0.0728	0.1826
6	0.8079 ± 0.0764	-0.0926	0.2378
8	0.7663 ± 0.0910	-0.1156	0.3050
10	0.7439 ± 0.0775	-0.1285	0.3443
12	0.7210 ± 0.1008	-0.1420	0.3870
14	0.7138 ± 0.0894	-0.1464	0.4010
16	0.6835 ± 0.1154	-0.1653	0.4631
18	0.6496 ± 0.1227	-0.1853	0.5394
20	0.6271 ± 0.1301	-0.2026	0.5946
22	0.6157 ± 0.1246	-0.2106	0.6242

TABLE 9

Isothermal annealing of 99.999% aluminium

Quenching temperature = 500°C

Annealing temperature = 10°C

Annealing Time Minutes	$(\frac{\Delta\epsilon}{\Delta\epsilon_o})$	$\log(\frac{\Delta\epsilon}{\Delta\epsilon_o})$	$(\frac{\Delta\epsilon_o}{\Delta t} - 1)$
0	1.0000	0.0000	0.0000
2	0.8248 ± 0.0331	-0.0836	0.2124
4	0.7247 ± 0.0443	-0.1398	0.3799
6	0.6811 ± 0.0487	-0.1668	0.4682
8	0.6373 ± 0.0448	-0.1956	0.5691
10	0.5936 ± 0.0342	-0.2265	0.6846
12	0.5623 ± 0.0650	-0.2500	0.7784
14	0.5186 ± 0.0580	-0.2852	0.9283
16	0.4749 ± 0.0278	-0.3234	1.1057
18	0.4436 ± 0.0357	-0.3530	1.2543
20	0.4310 ± 0.0473	-0.3655	1.3202
22	0.4047 ± 0.0361	-0.3929	1.4710

TABLE 10

Isothermal annealing of Al - 0.035 wt % Cr alloy

Quenching temperature = 500°C

Annealing temperature = 10°C

Annealing Time Minutes	$(\frac{\Delta\epsilon}{\Delta\epsilon_0})$	$\log(\frac{\Delta\epsilon}{\Delta\epsilon_0})$	$(\frac{\Delta\epsilon_0}{\Delta\epsilon} - 1)$
0	1.0000	0.0000	0.0000
2	0.8889 ± 0.0059	-0.05115	0.1250
4	0.8229 ± 0.0323	-0.0846	0.2152
6	0.7619 ± 0.0434	-0.1181	0.3125
8	0.7121 ± 0.0404	-0.1475	0.4043
10	0.6643 ± 0.0308	-0.1776	0.5053
12	0.6438 ± 0.0371	-0.1912	0.5533
14	0.6098 ± 0.0609	-0.2148	0.6399
16	0.5824 ± 0.0605	-0.2348	0.7170
18	0.5422 ± 0.0023	-0.2658	0.8443
20	0.5245 ± 0.0735	-0.2802	0.9066
22	0.4811 ± 0.0639	-0.3177	1.0786
24	0.4734 ± 0.0615	-0.3248	1.1124
26	0.4431 ± 0.0687	-0.3535	1.2568

TABLE 11

Isothermal annealing of 99.999% aluminium

Quenching temperature = 500°C

Annealing temperature = 20°C

Annealing Time Minutes	$(\frac{\Delta e}{\Delta e_o})$	$\log(\frac{\Delta \epsilon}{\Delta \epsilon_o})$	$(\frac{\Delta e_o}{\Delta e} - 1)$
0	1.0000	0.0000	0.0000
2	0.7666 ± 0.0177	-0.1154	0.3045
4	0.6865 ± 0.0188	-0.1634	0.4567
6	0.6064 ± 0.0263	-0.2172	0.6491
8	0.5268 ± 0.0218	-0.2783	0.8983
10	0.4731 ± 0.0218	-0.3250	1.1137
12	0.4401 ± 0.0124	-0.3564	1.2722
14	0.3735 ± 0.0482	-0.4277	1.6774
16	0.3134 ± 0.0661	-0.5039	2.1898
18	0.2534 ± 0.0660	-0.5962	2.9463
20	0.2000 ± 0.0816	-0.6990	4.0000

TABLE 12

Isothermal annealing of Al - 0.095 wt % Cr alloy

Quenching temperature = 500°C

Annealing temperature = 20°C

Annealing Time Minutes	$(\frac{\Delta e}{\Delta e_o})$	$\log(\frac{\Delta e}{\Delta e_o})$	$(\frac{\Delta e_o}{\Delta e} - 1)$
0	1.0000	0.0000	0.0000
2	0.8146 ± 0.0105	-0.0890	0.2276
4	0.6887 ± 0.0291	-0.1619	0.4520
6	0.5987 ± 0.0539	-0.2228	0.6703
8	0.5485 ± 0.0440	-0.2608	0.8232
10	0.5164 ± 0.0512	-0.2870	0.9365
12	0.5036 ± 0.0548	-0.2979	0.9857
14	0.4735 ± 0.0429	-0.3230	1.1039
16	0.4487 ± 0.0268	-0.3480	1.2287
18	0.4075 ± 0.0256	-0.3900	1.4540
20	0.3892 ± 0.0412	-0.4098	1.5694
22	0.3626 ± 0.0302	-0.4405	1.7579
24	0.3343 ± 0.0261	-0.4759	1.9913

TABLE 13

Isothermal annealing of 99.999% aluminium

Quenching temperature = 500°C

Annealing temperature = 30°C

Annealing Time Minutes	$(\frac{\Delta e}{\Delta \epsilon_o})$	$\log(\frac{\Delta \epsilon}{\Delta \epsilon_o})$	$(\frac{\Delta \epsilon_o}{\Delta \epsilon} - 1)$
0	1.0000	0.0000	0.0000
2	0.6805 ± 0.0290	-0.1672	0.4695
4	0.5419 ± 0.0180	-0.2660	0.8454
6	0.4573 ± 0.0293	-0.3400	1.1867
8	0.3549 ± 0.0688	-0.4499	1.8177
10	0.2534 ± 0.0310	-0.5962	2.9463
12	0.1631 ± 0.0330	-0.7875	5.1312
14	0.1025 ± 0.0365	-0.9892	8.7561

TABLE 14

Isothermal annealing of Al - 0.095 wt % Cr

Quenching temperature = 500°C

Annealing temperature = 30°C

Annealing Time Minutes	$(\frac{\Delta e}{\Delta e_o})$	$\log(\frac{\Delta e}{\Delta e_o})$	$(\frac{\Delta e_o}{\Delta e} - 1)$
0	1.0000	0.0000	0.0000
2	0.7710 ± 0.02.2	-0.1130	0.2970
4	0.6524 ± 0.0166	-0.1855	0.5328
6	0.5294 ± 0.0568	-0.2762	0.8889
8	0.4320 ± 0.0140	-0.3645	1.3148
10	0.3506 ± 0.0474	-0.4552	1.8523
12	0.3047 ± 0.334	-0.5161	2.2814
14	0.2479 ± 0.0371	-0.6057	3.0339

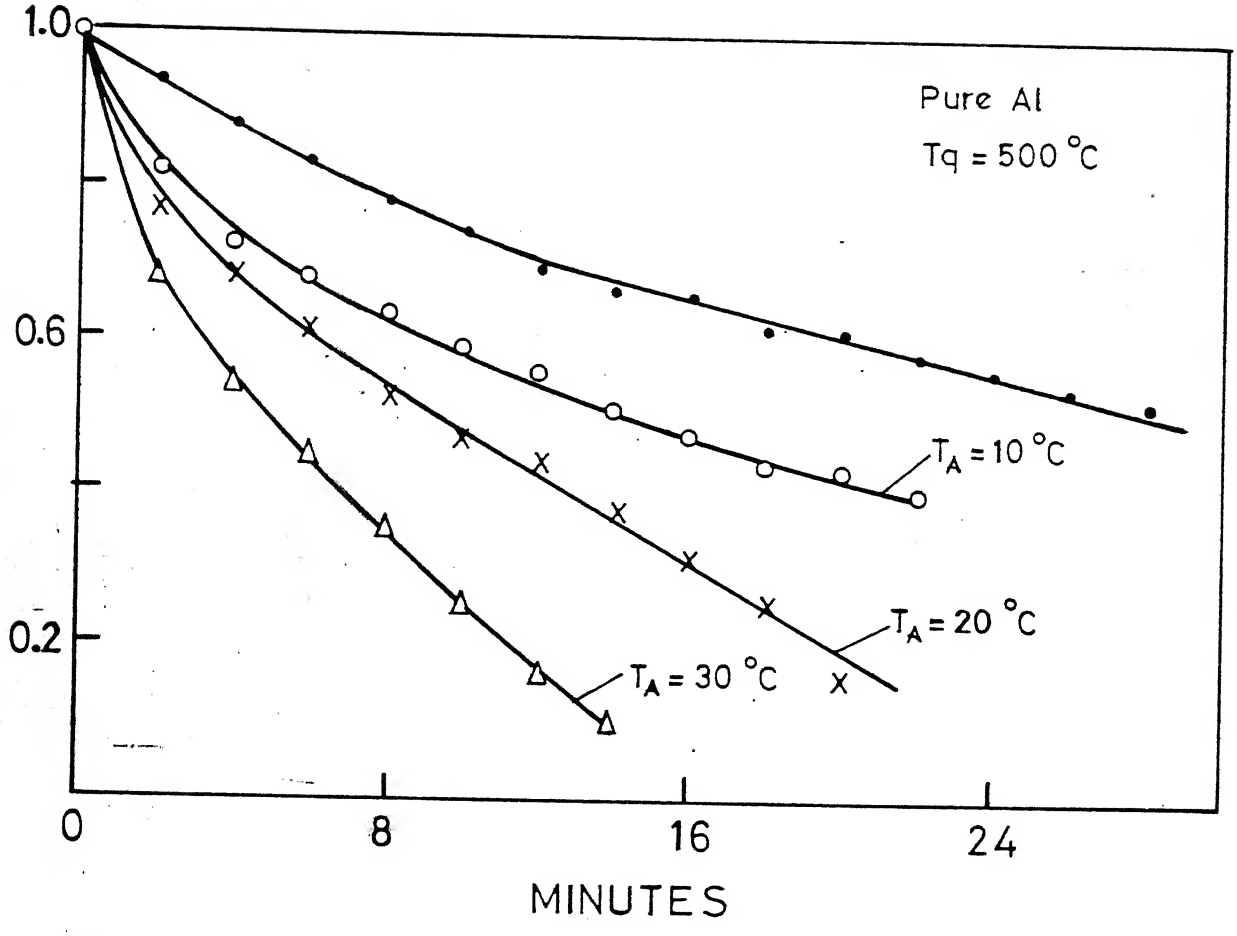

FIG. 7. ISOTHERMAL ANNEALING OF PURE Al

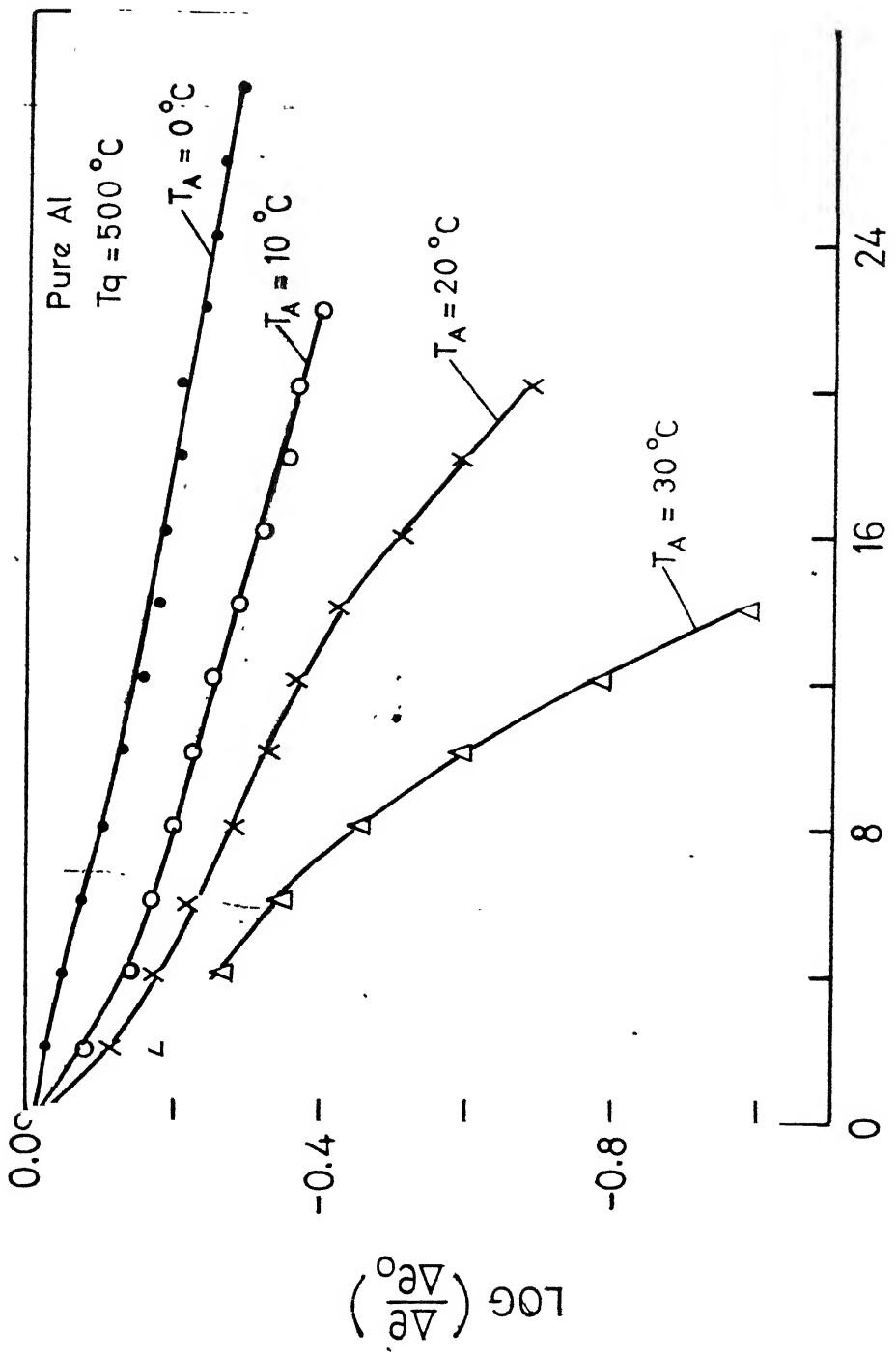

FIG.9 PLOT OF LOG $(\Delta e/\Delta e_o)$ VERSUS TIME FOR PURE Al

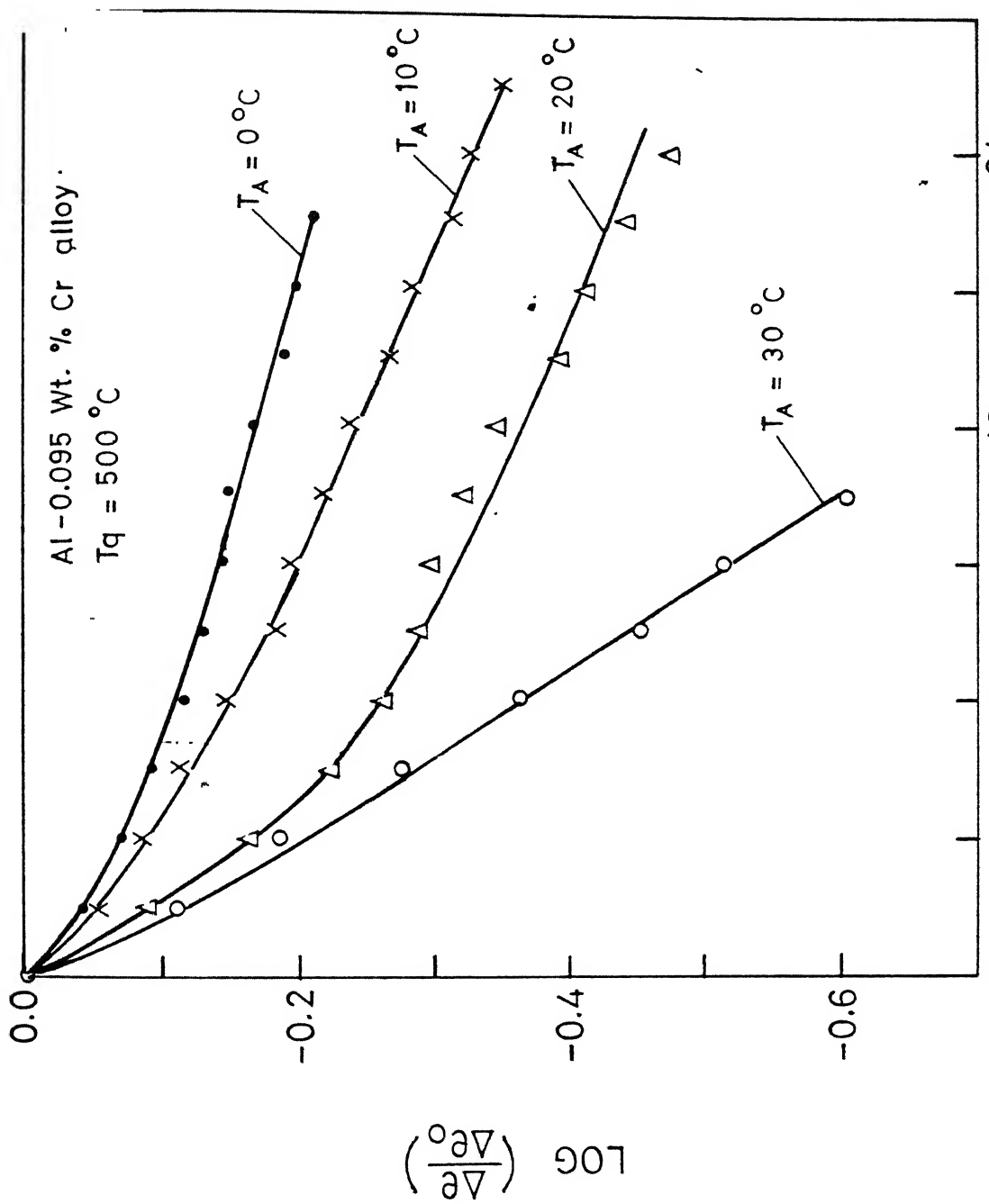

FIG.10 PLOT OF LOG $(\Delta e/\Delta e_o)$ VERSUS FOR Al-0 095 Wt % Cr ALLOY

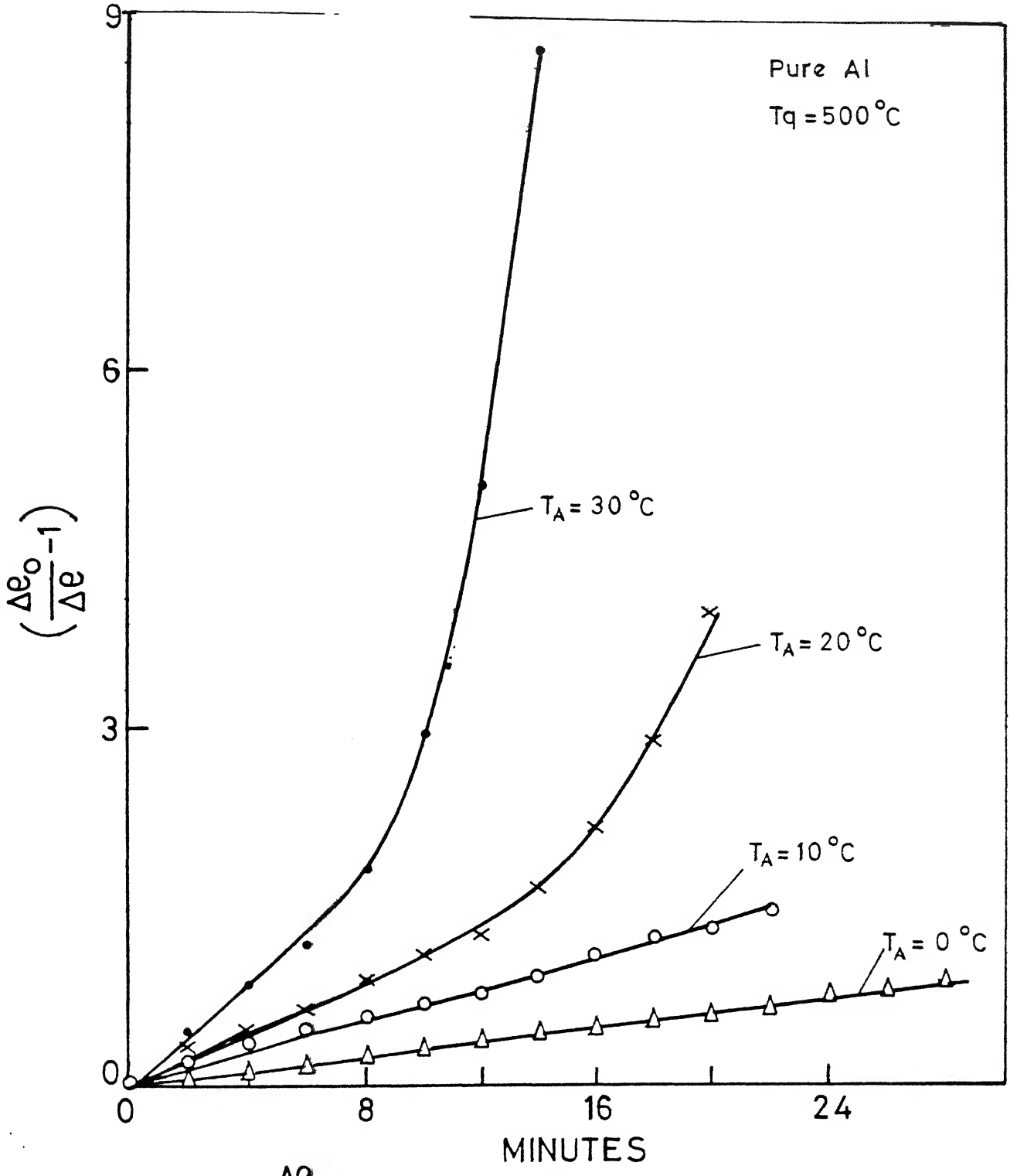

FIG.11 PLOT OF $\left(\frac{\Delta e_o}{\Delta e}-1\right)$ VERSUS TIME FOR PURE Al

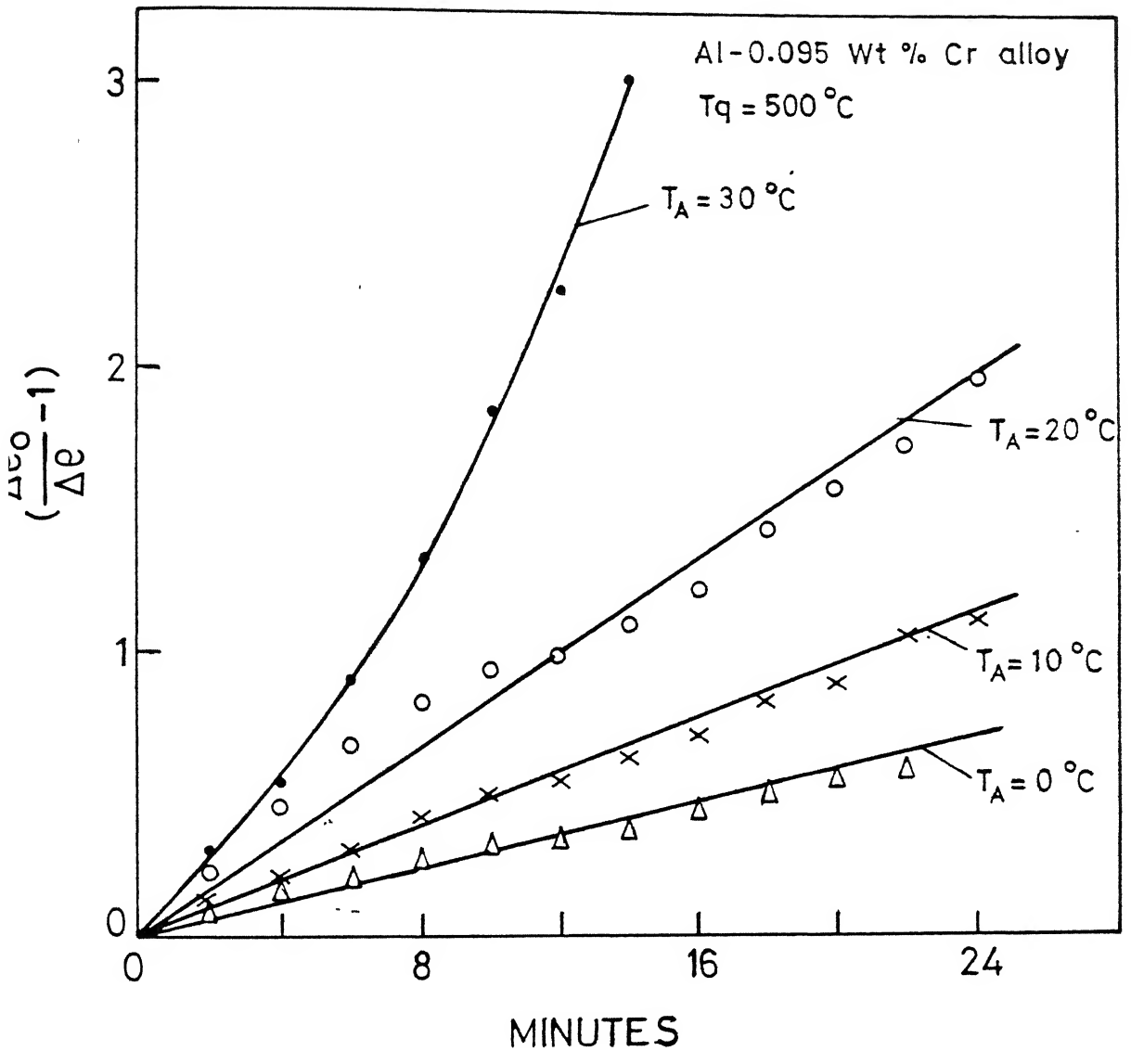

FIG.12 PLOT OF $(\frac{\Delta e_o}{\Delta e}-1)$ VERSUS TIME FOR Al-0.095 Wt % Cr ALLOY

$$\Delta\rho = \rho_t - \rho_f \tag{4.2}$$

$$\Delta\rho_o = \rho_q - \rho_f \tag{4.3}$$

where ρ_q = resistivity of the sample in the as quenched state

ρ_t = resistivity of the sample after annealing for t minutes

ρ_f = resistivity of the sample after annealing for 30 minutes at 70°C at the end of isothermal annealing. The final anneal of 30 minutes at 70°C has been chosen to ensure that Stage I is complete and the value for the resistivity obtained would then correspond to ρ_∞. (The resistivity after infinite time when the reaction corresponding to the first stage of recovery) in this experiment.

The errors in the values of $(\frac{\Delta\rho}{\Delta\rho_o})$ have also been indicated in the tables (7 to 14). It is seen that when the times for annealing are small, the error in the values of $(\frac{\Delta\rho}{\Delta\rho_o})$ are insignificant ($< 4\%$). However, for longer annealing times, the errors become significant ($\sim 15\%$).

The theory of annealing of vacancies in the pure metal has been out-lined in Chapter 2. If a low concentration of vacancies migrate to unfillable sinks, first order kinetics will be observed for the annealing process. In this case a plot of $\ln(\frac{\Delta\rho}{\Delta\rho_0})$ against time is a straight line with the slope equal to $-\alpha D$. From Figure 9, where the variation of $\ln(\Delta\rho/\Delta\rho_0)$ with time for the pure metal has been shown, it is clear that initially the plot is not linear; however, at large time, there is a tendency for the plot to be linear. As pointed out in Section 2.5, when vacancies anneal to sinks with simultaneous formation of solute-vacancy complexes and if the latter are immobile, a plot of $\ln(\frac{\Delta\rho}{\Delta\rho_0})$ against time is linear with the slope equal to $-K_e$. This plot for the alloy is shown in Figure 10. It has been seen that there is deviation from linearity in the early stages of annealing; however, in the later stages first order annealing kinetics have been observed.

Investigations on pure aluminium quenched from high temperature have shown[11,12] that second order annealing kinetics have been observed at least upto 60% of the annealing process. If the annealing process obeys second order kinetics then,

$$\frac{dV}{dt} = -KV^2 \qquad (4.4)$$

Integrating from the limits t = 0 to t = t,

$$\frac{V_o - V}{V\,V_o} = Kt \qquad (4.5)$$

where V_o is the concentration at time zero,

V is the concentration at time t,

K is the rate constant.

In terms of resistivities

$$\frac{\Delta\rho_o - \Delta\rho}{\Delta\rho \cdot \Delta\rho_o} = Kt \qquad (4.6)$$

Therefore, a plot of $(\frac{\Delta\rho_o}{\Delta\rho} - 1)$ against time is linear if second order annealing kinetics are obeyed. Figures 11 and 12 show such plots for pure aluminium and the alloy. In the case of pure aluminium, the plots for annealing temperatures of 0 and 10°C show linear behaviour whereas those for 20 and 30°C deviate from linearity. In a similar manner the annealing kinetics for the alloy at 0 and 10°C are of the second order. It is possible to fit the data for annealing at 20°C to second order kinetics. However, the data for annealing at 30°C shows deviation from second order kinetics.

The data for annealing of vacancies in the alloy have been analysed on the basis of simultaneous annealing of single and divacancies. The various equations given (2.32 and 2.33) have been solved on an IBM 7044 computer for number of values of B_{V-Cr} for isothermal annealing at 0, 10, 20 and 30°C.[28] The data relevant to the present set of results have been shown in table 15. The values for the various constants used in this calculation have been shown in the tables. In order to convert the values of N_o and N (N_o is the total number of vacancies at t = 0 and N that at time t) to $\Delta\epsilon_o$ and $\Delta\rho$, it has been assumed that the contribution of a divacancy to resistivity is twice that of a single vacancy and the solute vacancy complex contributes the same as a free vacancy. In this case

$$\frac{N}{N_o} = \left(\frac{\Delta\rho}{\Delta\rho_o}\right) \qquad (4.7)$$

Computer produced plots of $\left(\frac{\Delta\rho}{\Delta\rho_o}\right)$ against time have been shown in Figures 13 to 16. The experimental points are compared with the theoretical curves to calculate the binding energy. The results have been tabulated in table 16.

TABLE 15

Solution of differential equation (2.23) to (2.25) IBM 7044

Values of some of the parameters used:

$E_V^f = 0.76$ eV ; $T_q = 773$ °K

$\nu = 10^{13}$/sec; $k = 8.62 \times 10^{-5}$ eV

$\alpha = 10^{10}$; $E_{m(2)} = 0.50$ eV

$E_{m(1)} = 0.60$ eV; $\lambda = 2.86$ Å

$B_2 = 0.17$ eV; $I_o = 5 \times 10^{-4}$ at.fr.

I. Annealing temperature = 273°K

$B_{V-Cr} = 0.013$ eV		Time	$B_{V-Cr} = 0.15$ eV	
N x 10^5	N/N_o	secs.	N x 10^5	N/N_o
1.16192	1.000	0	1.17838	1.000
1.13704	0.978	30	1.16778	0.991
1.11103	0.956	60	1.15772	0.982
1.086465	0.935	90	1.14797	0.974
1.06285	0.915	120	1.13835	0.966
1.040144	0.895	150	1.12888	0.957
1.01828	0.876	180	1.11954	0.950
0.99721	0.858	210	1.11103	0.943
0.97692	0.840	240	1.10125	0.934
0.95735	0.824	270	1.09231	0.927
0.93845	0.808	300	1.08348	0.920
0.92021	0.792	330	1.07478	0.912
0.90257	0.777	360	1.06619	0.905
0.88554	0.762	390	1.05772	0.897
0.86905	0.748	420	1.04937	0.890
0.85309	0.734	450	1.04112	0.883
0.83766	0.721	480	1.03300	0.876

Continued...

TABLE 15 (Continued)

II. Annealing temperature = 283°K

B_{V-Cr} = 0.14 eV		Time secs.	B_{V-Cr} = 0.15 eV	
N x 10^5	N/N_o		N x 10^5	N/N_o
1.16952	1.000	0	1.17838	1.000
1.13061	0.967	30	1.1530	0.978
1.09294	0.934	60	1.1284	0.958
1.05794	0.905	90	1.1051	0.938
1.02482	0.876	120	1.0826	0.919
0.99344	0.849	150	1.0608	0.900
0.96365	0.824	180	1.0397	0.882
0.93533	210	210	1.0194	0.862
0.90840	0.777	240	0.9997	0.848
0.88276	0.755	270	0.9806	0.832
0.858296	0.734	300	0.9621	0.816
0.83495	0.714	330	0.9442	0.801
0.81264	0.695	360	0.9268	0.787
0.79131	0.676	390	0.9099	0.772
0.77423	0.662	420	0.8936	0.758
0.75131	0.642	450	0.8777	0.745
0.73256	0.626	480	0.8622	0.731

Continued...

TABLE 15 (Continued)

III. Annealing temperature = 293°K

B_{V-Cr} = 0.15 eV

Time secs.	N x 10^5	N/N_o
0	1.17838	1.000
30	1.12092	0.951
60	1.06722	0.906
90	1.01834	0.864
120	0.97293	0.826
150	0.93075	0.790
180	0.89137	0.756
210	0.85453	0.725
240	0.82005	0.696
270	0.78768	0.668
300	0.75722	0.643
330	0.72857	0.618
360	0.70152	0.595
390	0.67599	0.574
420	0.65781	0.553
450	0.62891	0.534
480	0.60721	0.515

Continued...

TABLE 15 (Continued)

IV. Annealing temperature = 303°K

Time	B_{V-Cr} = 0.15 eV		B_{V-Cr} = 0.16 eV		B_{V-Cr} = 0.17 eV	
secs.	N x 10^5	N/N_o	N x 10^5	N/N_o	N x 10^5	N/N_o
0	1.1784	1.000	1.1885	1.000	1.2006	1.000
30	1.0580	0.898	1.1046	0.929	1.1438	0.953
60	0.9544	0.810	1.0284	0.865	1.0304	0.908
90	0.8671	0.736	0.9717	0.818	1.0415	0.867
120	0.7913	0.672	0.8998	0.757	0.9956	0.829
150	0.7250	0.615	0.8531	0.718	0.9526	0.793
180	0.6665	0.566	0.7935	0.668	0.9121	0.760
210	0.6147	0.522	0.7470	0.628	0.8740	0.728
240	0.5684	0.482	0.7043	0.593	0.8381	0.698
270	0.5270	0.447	0.6650	0.560	0.8043	0.670
300	0.4896	0.415	0.6287	0.529	0.7722	0.643
330	0.4558	0.387	0.5950	0.501	0.7419	0.618
360	0.4250	0.361	0.5638	0.474	0.7132	0.594
390	0.3970	0.336	0.5347	0.450	0.6860	0.576
420	0.3714	0.315	0.5076	0.427	0.6600	0.550
450	0.3479	0.295	0.4823	0.406	0.6355	0.529
480	0.3264	0.276	0.4587	0.386	0.6121	0.510

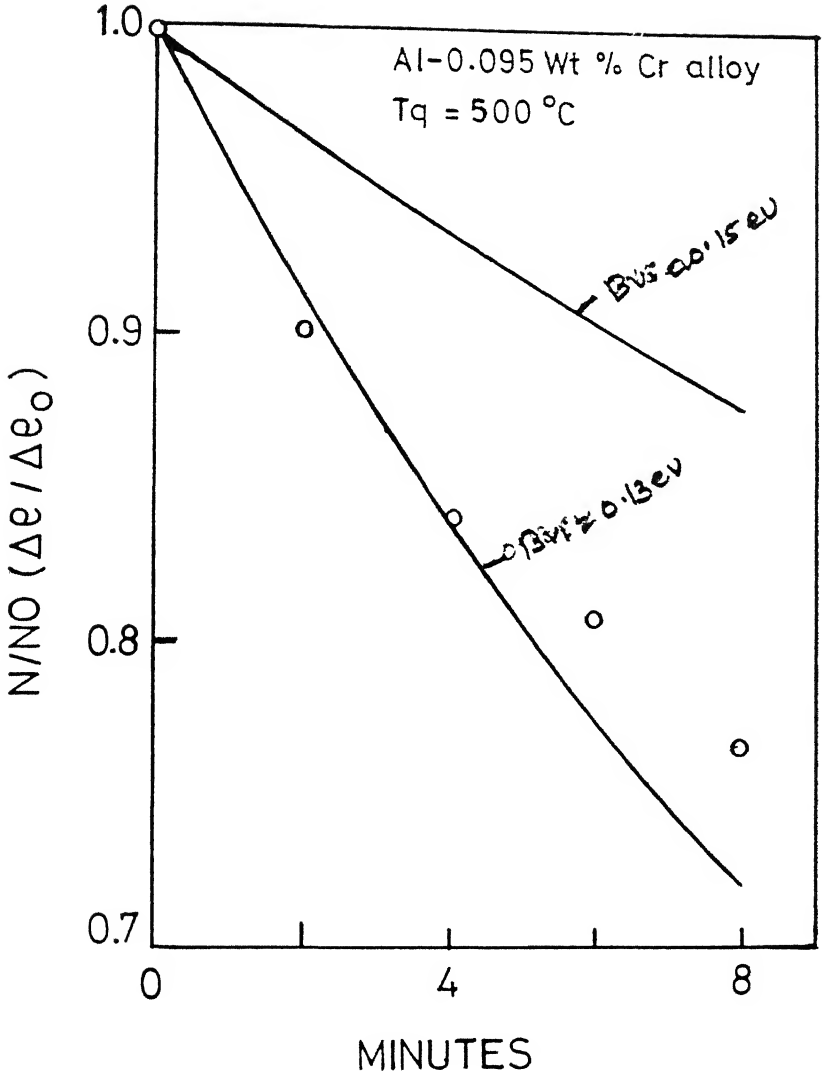

FIG.13 COMPARISON OF CALCULATED AND EXPERIMENTAL DATA FOR $T_A = 273\,^{\circ}K$

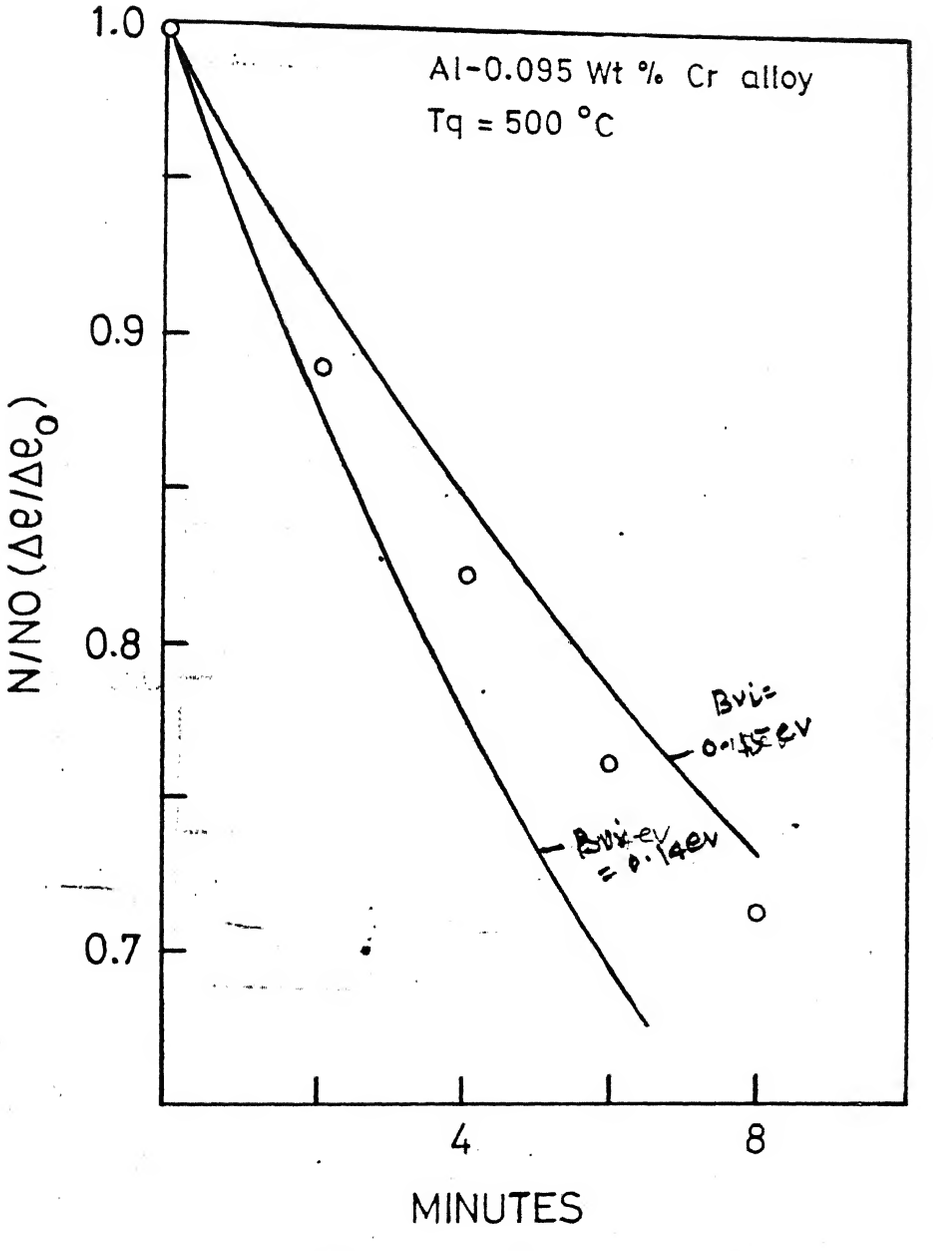

FIG.14 COMPARISON OF CALCULATED AND EXPERIMENTAL DATA FOR $T_A = 283\,^{\circ}K$

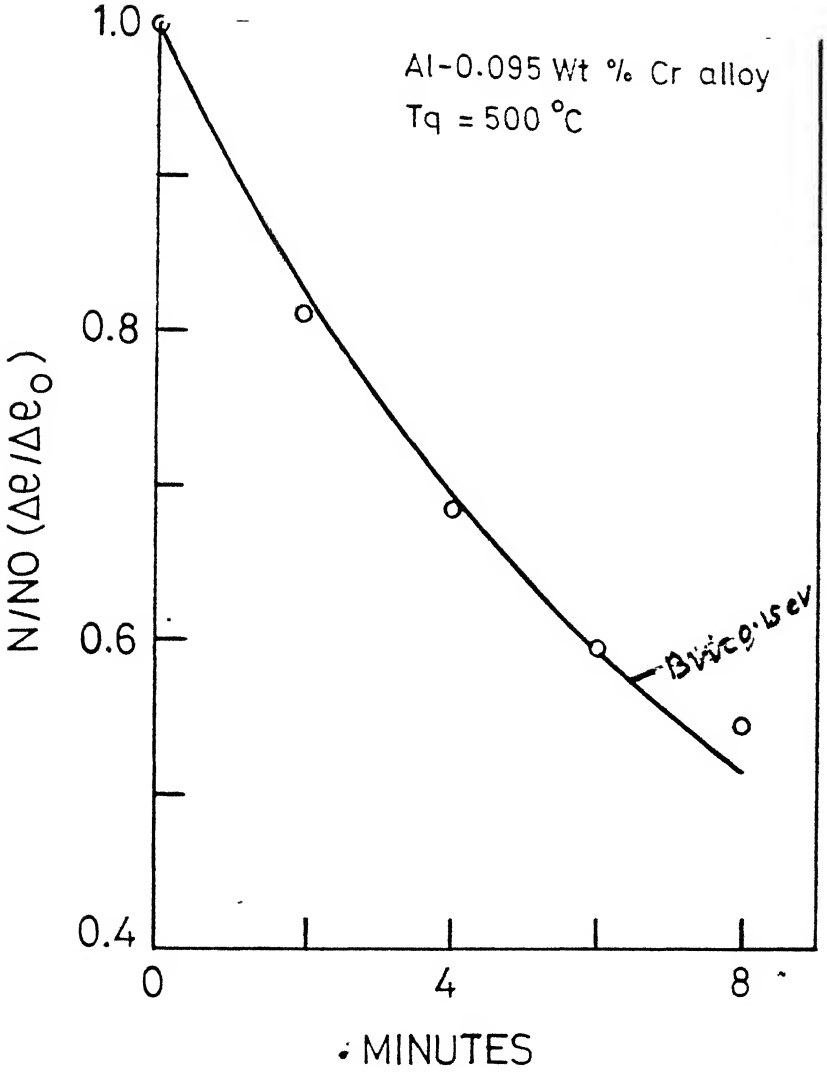

FIG.15 COMPARISON OF CALCULATED AND EXPERIMENTAL DATA FOR $T_A = 293\ ^{\circ}K$

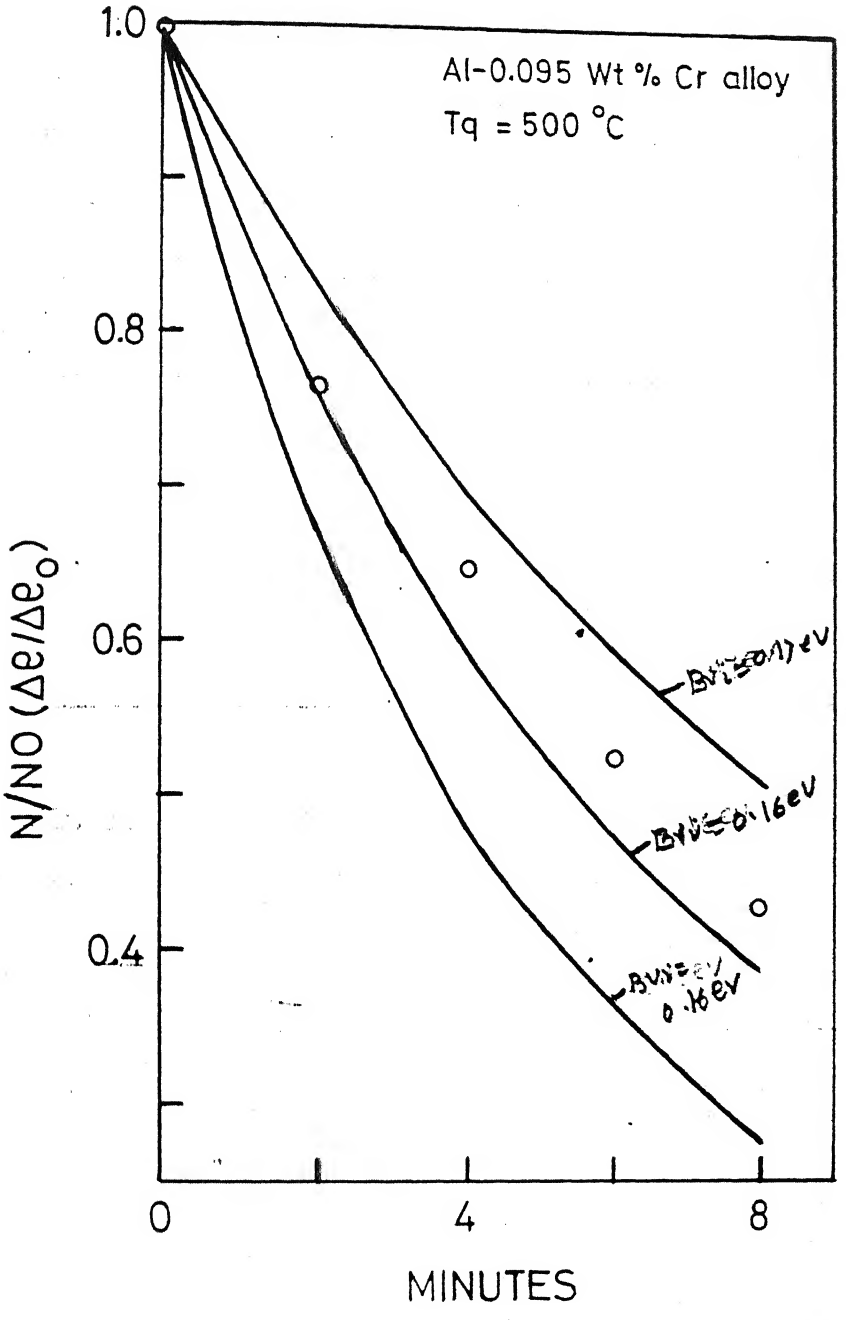

FIG.16 COMPARISON OF CALCULATED AND EXPERIMENTAL DATA FOR $T_A = 303\,^{\circ}K$

TABLE 16

Calculated values of the chromium-vacancy binding energy at different annealing temperatures

Annealing Temperature °K	B_{V-Cr}, eV
273	Close to 0.13
283	0.14 - 0.15
293	0.15
303	0.16 - 0.17

It is seen that the chromium-vacancy binding energy lies in the range 0.13 to 0.17 eV.

4.5 ISOTHERMAL ANNEALING OF THE QUENCHED ALLOY AT 250°C:

To check whether any precipitation has occurred when the quenched alloy has been annealed at temperature of the order of 200-250°C, isothermal annealing treatment of the alloy has been carried out at 250°C. The resistivity measurements have been made until there is no change in resistivity with time. The data for 250°C annealing has been shown in table 17, and plotted in Figure 17. The relation used in this plot is given by,

TABLE 17

Isothermal annealing of quenched Al - 0.095 wt % Cr alloy

Quenching temperature = 500°C

Annealing temperature = 250°C

$\Delta\rho = \rho_q - \rho_t$

Annealing time t, minutes	$\Delta\rho$ n ohm cm
10	12.1
40	30.0
100	50.7
220	78.2
310	96.3
460	111.7
640	123.8
820	134.9
1060	144.5
1195	150.0
1360	151.4
1525	151.4

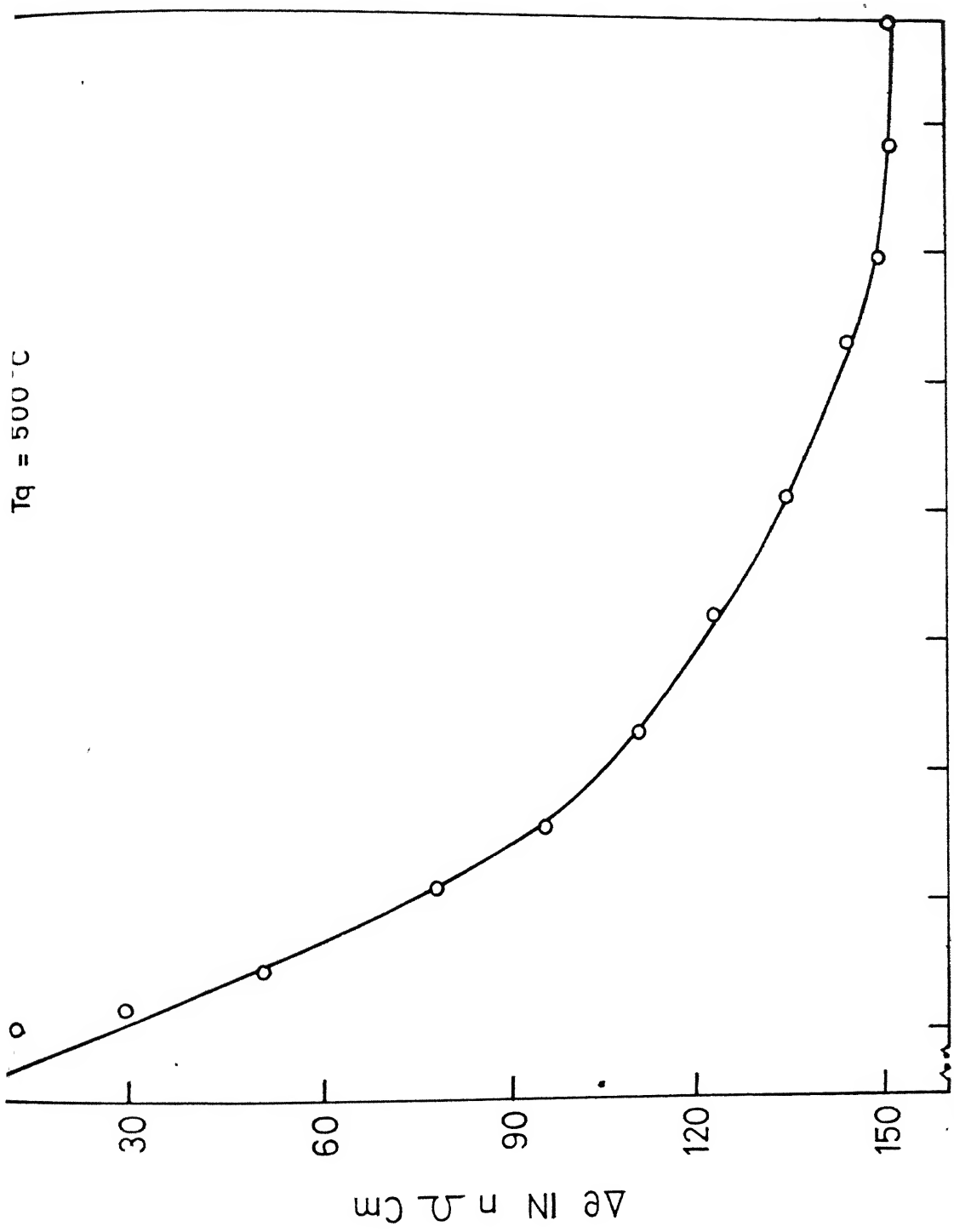

FIG.17 ISOTHERMAL ANNEALING OF QUENCHED Al-0.095 Wt% Cr ALLOY AT 250 °C

$$\Delta\rho = \rho_q - \rho_t \qquad (4.1)$$

where ρ_q is the as-quenched resistivity, ρ_t is the resistivity after annealing for time t and $\Delta\rho$ is the excess resistivity.

The results indicate that the precipitation process has been completed in about 1200 minutes. The resistivity fall after the completion of this reaction is about 150 n ohms cm. This corresponds to precipitation of about $\frac{150 \times 10^{-9}}{8.66 \times 10^{-6}}$ at.% i.e. 0.017 at.% chromium. More work needs to be done in this region to thoroughly investigate the precipitation kinetics.

CHAPTER 5

CONCLUSION

The following conclusions have been drawn from the present investigation.

(1) The contribution to resistivity of chromium dissolved in aluminium is of the order 8.66 micro-ohm/at%.

(2) The isochronal annealing curves for pure aluminium and aluminium - 0.095 wt % chromium quenched from 500°C are similar. There are two recovery stages in the interval 0 to 50°C and 140 to 220°C for pure aluminium whereas for the alloy, these stages are from 0 to 40°C and 120 to 240°C.

(3) The isothermal annealing kinetics of pure aluminium and aluminium - 0.095 wt % chromium alloy quenched from 500°C and annealed in the temperature range 0 to 30°C do not follow the first order kinetics. The low temperature annealing curves can be fitted to second order kinetics.

(4) With the help of model which considers the simultaneous annealing of both single and divacancies, the chromium vacancy binding energy has been found to be in the range 0.13 to 0.17 eV.

(5) When the alloy is quenched from 500°C and then annealed at 250°C, there is an appreciable fall in resistivity of the order of 150 n ohms cm. which must be associated with the precipitation of chromium. This needs more extensive investigation.

REFERENCES

1. R.P. Johnson, Phys. Rev., 56, 814 (1939).
2. T. Federighi, "Lattice Defects in Quenched Metals", (Academic Press), 217 (1965).
3. G.M. Hood and R.J. Schultz, Phil. Mag., 23, 1479 (1971).
4. W.M. Lomer, "Vacancies and Other Point Defects in Metals and Alloys", Institute of Metals, 79 (1958).
5. M. Kiritani, J. Phys. Soc. Japan 19, 618 (1964).
6. M. Doyama, "Lattice Defects in Quenched Metals", P. 167 (1965).
7. M. Doyama, Phys. Rev., 148, 681 (1966).
8. C. Panseri and T. Federighi, Phil. Mag., 3, 1223 (1958).
9. J. Silcox and M.J. Whelan, Phil. Mag., 5, 1 (1960).
10. J. Burke and T.R. Ramachandran, Metal Science J., 5, 223 (1971).
11. W. Desorobo and D. Turnbull. Phys. Rev., 115, 560 (1959).
12. M. Doyama and J.S. Koehler, Phy. Rev., 134, A522 (1964).
13. A.C. Damask and G.J. Dienes, "Point Defects in Metals", (Gordon and Breach, New York), (1963) p. 110.
14. A.C. Damask and G.J. Dienes, Phys. Rev. 120, 99 (1960).
15. A.C. Damask and G.J. Dienes, Acta. Met., 12, 797 (1964).
16. K.P. Chik, "Vacancies and Interstitials in Metals", (North-Holland Publishing Co., Amsterdam), 183 (1969).

17. D.P. Lahiri, Ph.D. Thesis, I.I.T. Kanpur (1973).

18. Vijendra Singh, M.Tech. Thesis, I.I.T. Kanpur (1975).

19. D.P. Lahiri, T.R. Ramachandran and A.K. Jena, Trans. Ind. Inst. Metal, 27(6), 360 (1974).

20. K. Nagahama, I. Miki, Trans. J.I.M., 15(3), 185 (1974).

21. R.P. Elliott, "Constitution of Binary Alloys, First Supplement", (McGraw Hill), P. 33 (1969).

22. M. Hansen, "Constitution of Binary Alloys, Second Supplement", (McGraw Hill), P. 29 (1969).

23. "Bulletin on Precision Kelvin Bridge", by Leads and Northup Co., Philadelphia, U.S.A., P. 6 (1961).

24. G.T. Meaden, "Electrical Resistance of Metals", P. 147 (1965).

25. F.H. Harris, "Electrical Measurements", (John Wiley, New York), P. 264 (1962).

26. "Instruction Manual" - Fischer Scientific, New York, U.S.A.

27. F.J. Kedves, L. Gergely, M. Hordos and E. Kovacs Csetenyi, Phys. Stat. Solidi (a), 13, 685 (1972).

28. T.R. Ramachandran, unpublished work (1973).